

STRENGTH ENHANCEMENT OF CONCRETE CONTAINING MSW INCINERATOR ASH

James T. Cobb, Jr., Daniel J. Reed and James T. Lewis III
Department of Chemical & Petroleum Engineering
University of Pittsburgh
Pittsburgh, Pennsylvania 15261

Keywords: municipal solid waste, incinerator ash, concrete

ABSTRACT

In previous work [1] pretreatment of fresh municipal solid waste (MSW) incinerator ash with a novel type of additive, which was not identified chemically in that paper, was shown to markedly increase the compressive strength of portland cement concrete using the MSW ash as fine aggregate. A recent study has shown that, at lower levels of additive, aged MSW ash does not demonstrate the same enhancement. This presentation will provide additional information concerning the previous study, give the results of the current one and discuss the implications of both.

INTRODUCTION

Much work is being conducted to find beneficial uses for the solid residues from energy-conversion process, such as coal-fired electric power plants and combustors of municipal solid waste (MSW). Landfill caps and liners, grouts, structural fills, artificial aggregate for road bases, concretes of various types, and additives for cement have all been examined as outlets for these energy-related wastes. For all of the uses just listed, solidification is the principal goal, while stabilization of the eight RCRA metals (arsenic, barium, cadmium, chromium, lead, mercury, selenium and silver) is an important secondary consideration.

Two residues obtained from the most thorough of the MSW combustors - the O'Conner rotary burner - fail to meet the following specifications for Class C Fly Ash - moisture content, ignition loss, pozzolanic activity index and fineness. [1] In addition they fail the EP toxicity test for cadmium and lead [1], as shown in Table 1. Thus, they cannot be used as cement additives and they must be stabilized when included in any of the other beneficial uses listed in the last paragraph.

An earlier paper [1] described a study in which a combined MSW ash from the O'Conner combustor was used as fine aggregate in portland cement concrete. In that paper it was pointed out that using MSW ash for this purpose substantially degrades the strength of the concrete so produced, but it reported that a novel additive had been discovered which gives early indications of economically restoring concretes containing MSW ash to their normal strengths.

However, the authors of that earlier paper did not reveal the chemical composition of the novel additive. At that time they were exploring the possibility of obtaining a patent on the use of the additive. Since then, they have decided that, such a patent being essentially be unenforceable if awarded, the nature of the additive should be disclosed.

One purpose of this paper, then, is that disclosure, along with some additional information obtained during the last few months of the Westinghouse-sponsored project, which came to its conclusion shortly after that paper was written. [2] Subsequently, another graduate student conducted a brief examination of this topic and found some interesting differences between the behavior of fresh and aged MSW ash. [3] The second purpose of this paper, then, is to report his findings.

SOLIDIFICATION ENHANCEMENT USING NOVEL ADDITIVES

The novel additive is a common acid. Two different acids have been tested - hydrochloric acid and acetic acid. The method of introduction of the acid may best be shown by giving the procedure (based upon ASTM C192-88) for mixing a batch of concrete in which it is included. The specific batch described is Batch 32:

- Add 17.0 pounds of coarse aggregate and 25.8 pounds of MSW ash to a small cement mixer and commence rotation.
- Add 500 ml of 12 normal hydrochloric acid and mix for several minutes.

- Add 33.5 pounds of cement and 12.0 pounds of water (enough to provide a slump of 1.5 to 2.5 inches) to the mixer in equal proportions, one after the other, in three or four different intervals.
- When the mix is ready for molding, fill twenty three inch by six inch cylindrical cardboard molds and place them in a curing room.
- After each period of three, seven, fourteen, twenty-eight and ninety days, test four cylinders for compressive strength, reporting the average strength of the strongest three cylinders.

Figure 1 provides a record of the 28-day average compressive strengths for twelve concretes prepared with MSW ash as fine aggregate and with varying amounts of either hydrochloric acid or acetic acid. The abscissa is structured in units of gram moles/pounds MSW ash. For comparison, the 28-day strength of a concrete made with no additive (Batch 5) is shown. Nearly a 300% increase in compressive strength (1400 psi to 5500 psi) is achieved by Batch 30, made with 0.25 gram moles of hydrochloric acid per pound of MSW ash.

The results of the 90-day compressive strengths are confused. These batches were made near the end of the project and 90-day strengths were not obtained for Batches 44 through 49. In addition, the cylinders for Batches 27, 35, 36 and 37 deteriorated such that no strength could be measured. The 90-day compressive strengths for Batches 30, 31, 32 and 42 are 4940, 4380, 6200 and 1618 respectively. [It should be noted that no 28-day strength for batch 42 was measured. The value in Figure 1 is the 90-day strength.] Thus, the compressive strength of Batch 30 decreased somewhat after Day 28, that for Batch 31 rose very slightly and that for Batch 32 increased dramatically. The addition of these two acids may be affecting the crystallography of the cementitious portion of the concretes. Intermediate amounts of acid appear to increase strength without degradation, while larger amounts cause deterioration. Much work needs to be conducted to understand the causes and effects of strength enhancement by acid addition.

METAL STABILIZATION IN MSW ASH-CONTAINING CONCRETE

Samples of the first nine concretes containing MSW ash, made in this project, were extracted by the project team according to the EP toxicity method and the concentrations of the eight RCRA metals in the extracts were measured by Geochemical Testing of Somerset, Pennsylvania. The results of these tests are given in Table 1. The two metals, cadmium and lead, which caused the MSW ash to fail the EP toxicity test, have been well stabilized in all nine concretes.

COMPARISON OF BEHAVIOR OF FRESH AND AGED ASH

This portion of the study was conducted two years after the earlier portion. Aged ash was drawn from the fourth (and final) batch of ash that had been collected several years previously. Fresh ash was obtained from the Dutchess County MSW Incinerator. It was drawn from the ash conveyor prior to lime addition.

This portion of the study utilized mortar, rather than full concrete containing coarse aggregate. The method of mortar production, based upon ASTM C109, was as follows:

- Place the ash into a mixing bowl.
- Add hydrochloric acid (if it is to be used) and mix.
- Add water and mix.
- Add cement (to a water/cement ratio of 0.81) and mix.
- Fill six plastic two-inch molds with mortar, place them in a curing room for 24 hours, break them from the molds, and continue curing for six more days.
- Measure the compressive strength of each of the six cubes, using a universal testing machine; calculate the average strength of the four strongest cubes.

Figure 2 provides a record of the compressive strengths for eight aged ash-containing mortars, six prepared with varying amounts of hydrochloric acid and two with no acid. Figure

3 provides a record of the compressive strengths for three fresh ash-containing mortars, two prepared with varying amounts of hydrochloric acid and one with no acid. For comparison of Figures 2 and 3 with Figure 1, it may be noted that 100 mmol of acid in Figures 2 and 3 corresponds to 0.032 gram moles acid/pound of ash in Figure 1.

First, it may be observed that all of the mortars were prepared with relatively low amounts of acid. The largest amount of acid, about 0.05 gram moles acid/pound of ash, was used in Batch 6. This corresponds to the amount used in Batches 31 and 37 of the earlier portion of the study. Thus, the increases in compressive strength with increasing amounts of acid, observed in Figures 2 and 3 to be under 100%, are as expected, based upon the experience recorded in Figure 1.

From a comparison of Figures 2 and 3 it is clear that the compressive strength of mortar made from fresh ash is over six times that of mortar made from aged ash. Fresh ash has a certain amount of pozzolanic character which is lost as it ages. It is also clear from this comparison that acid addition is much more effective in increasing the compressive strength of mortar containing fresh ash than for that containing aged ash. Mortar with fresh ash doubles in strength with the addition of about 60 mmols of acid, while mortar with aged ash may require 120 mmols or more of acid for the same effect. Thus, there may be a phenomenological linkage between the strength enhancement caused by acid addition and the pozzolanic nature of the ash.

CONCLUSIONS

The addition of common acids, such as hydrochloric and acetic acids, to mortars and concretes containing MSW incinerator ash, increases the compressive strength of the final product. The increase is more pronounced when the ash is fresh. Aging of ash degrades the final strength of the mortar and also reduces the effect to be expected by acid addition.

It should be noted that the results of this study are quite preliminary in nature. Much more work needs to be done to verify and quantify the trends and to ascertain their causative mechanism.

REFERENCES

- [1] Cobb, J. T., Jr., et al., *Clean Energy from Waste & Coal*, M. R. Khan, ed., ACS Symposium Series, 515, 1993, p. 264.
- [2] Reed, D. J., MS Thesis, University of Pittsburgh, 1992.
- [3] Lewis, J. T., III, MS Thesis, University of Pittsburgh, 1994.

Constituent	EP-toxicity Maximum Allowable Limit	Primary Drinking Water Standards	Plain Concrete Control A/B	Avg Concrete Samples 1 to 9	Max. Concrete Samples 1 to 9	Avg Ash Samples 1 and 2	Max. Ash Samples 1 and 2
Arsenic	5.00	0.050	0.006	0.0192	0.05	0.011	0.019
Barium	100.00	1.000	1.09	0.7600	1.36	0.195	0.240
Cadmium	1.00	0.010	0.01	0.1067	0.47	1.375	1.770
Chromium	5.00	0.050	0.09	0.0333	0.09	0.04	0.050
Lead	5.00	0.050	0.01	0.1522	0.78	6.08	7.480
Mercury	0.20	0.002	0.0002	0.0007	0.004	0.001	0.001
Selenium	1.00	0.010	0.002	0.0042	0.02	0.002	0.002
Silver	50.00	0.050	0.01	0.0167	0.03	0.025	0.030

Table 1. EP Toxicity Tests on Nine Concretes Containing MSW Ash

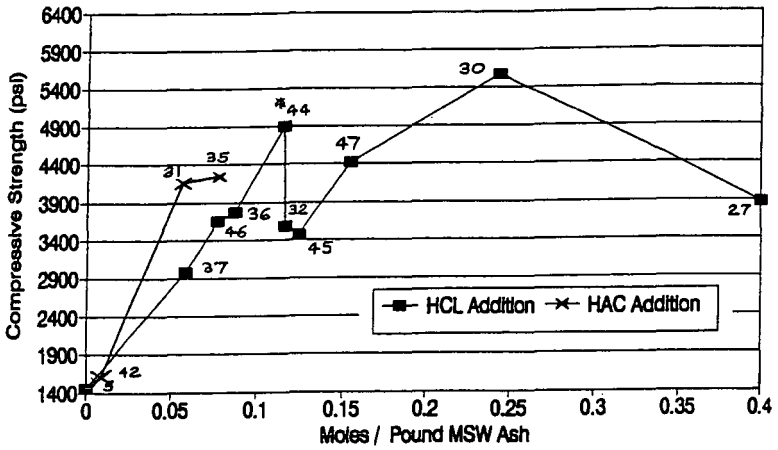


Figure 1. Effect of Acid Concentration on Compressive Strength of Concrete Containing MSW Ash

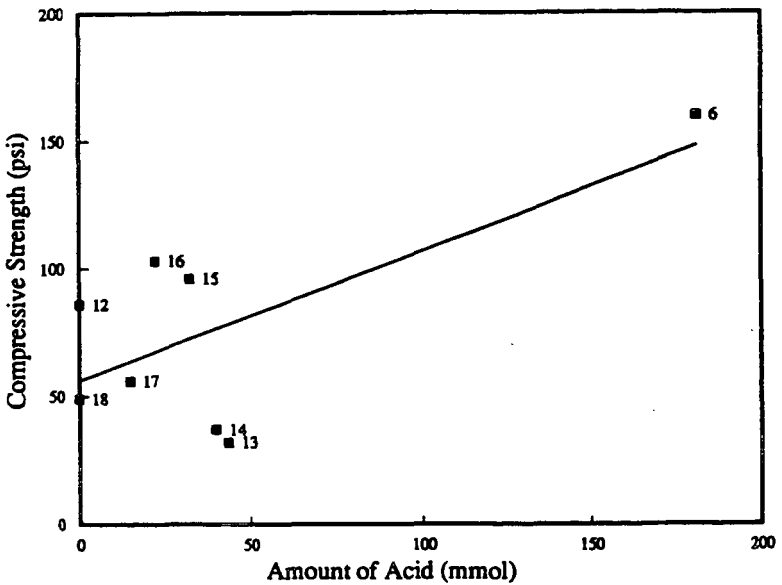


Figure 2. Effect of Acid Concentration on Compressive Strength of Mortar Containing Aged MSW Ash

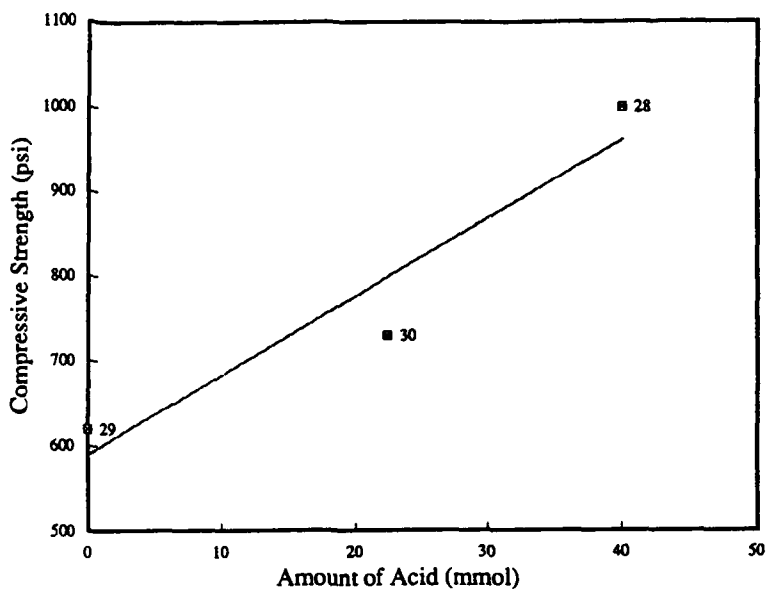


Figure 3. Effect of Acid Concentration on Compressive Strength of Mortar Containing Fresh MSW Ash

INVESTIGATION OF THE CO₂ ABSORPTION CAPACITY OF DRY FGD WASTES.

Taulbee, D.N., Graham, U., Rathbone, R.F., and Robl, T.L.
University of Kentucky-Center for Applied Energy Research
3572 Iron Works Pike
Lexington, KY 40511

Keywords: CO₂ or carbon dioxide, Flue-gas desulfurization or FGD, natural gas, Calcium Oxide

ABSTRACT

Numerous utility boilers and tail-gas desulfurization units utilize lime or limestone-based sorbents to remove sulfur oxides generated during the combustion of fossil fuels. Such units generate about 20 million tons of flue-gas desulfurization (FGD) wastes annually in the U.S., the bulk of which (~95%) is discarded in landfills or holding ponds.¹ Thus, commercial utilization of FGD wastes would benefit from both a plentiful low-cost raw material as well as a significant savings in disposal. One such use may be for the reduction of CO₂ in multi-component gas streams.

During the removal of SO₂, the lime added to or generated in the desulfurization unit, is not fully utilized. That is, a portion of the Ca fed to the unit is not sulfated (remains as CaO or Ca(OH)₂). In some FGD wastes, the fraction of available Ca is quite high (> 1/3), particularly for dry wastes. When hydrated, such wastes exhibit a strong affinity to absorb CO₂ at ambient temperature. Further, both the kinetics and extent of absorption are favorable as CO₂ initially at ~2.5 volume% was rapidly reduced to below the detection limit of the measurement device (ppm range) used in this study. Leaching behavior and changes in the mineralogy of the FGD samples exposed to CO₂ are also discussed.

INTRODUCTION.

Over the past decade, numerous FGD units have been added to existing utility boilers in an effort to satisfy federal mandates on SO₂ emissions. Such units are usually classified as either wet or dry depending on whether the absorbent is used in a slurry (wet) or as a hydrated solid. Wet scrubbers capture sulfur chiefly as gypsum (CaSO₄·H₂O) with some sulfite formation (e.g., CaSO₃·2H₂O). Dry technologies such as AFBC produce a dry product in which sulfur is captured mostly as anhydrite-CaSO₄ or for the dry tail-gas units such as spray drier and duct-injection, sulfur is captured as gypsum, anhydrite or hemi-hydrate (CaSO₄·H₂O). Dry FGD by-products also differ from their wet-scrubber counterparts in that a significant portion of the calcium in the dry waste remains unsulfated. This Ca is present as either calcium oxide, CaO, or as slaked lime, Ca(OH)₂. Because FGD wastes, particularly dry FGD wastes represent relatively new materials, <6% of the ~20 M tons of FGD wastes generated in 1993 are currently finding commercial uses.¹

The work described here represents a preliminary examination of the capacity of dry-FGD wastes to remove CO₂ from multi-component gas streams. Such an absorbent may have numerous commercial uses, e.g., gas purification, removal of CO₂ during H₂ production, etc. However, the current study focused on the potential to reduce CO₂ in simulated natural-gas streams. As a rule of thumb, the costs associated with available CO₂-removal technologies (wet scrubbers, molecular sieves, membranes) are prohibitive for gas wells that produce less than about 100,000 SCF/day.² This effectively eliminates commercial production from low-porosity, carbonate-containing strata common to many gas-producing deposits. Thus, a low-cost CO₂ absorbent that can be safely disposed or marketed (road base or fertilizer) may have applications in the natural-gas industry.

In this study, CO₂ absorption capacity was evaluated for waste samples generated from different utility boilers, one demonstration plant, and tests conducted under four sets of conditions in a single pilot plant. With the exception of a utility-derived fly ash used as a control, all samples examined are dry-FGD waste materials. Absorption capacity was examined for both hydrated samples as well as aqueous slurries. As of this writing, only gas blends containing inert gases and CO₂ or inert gas and CO₂/CH₄ have been tested. Additional tests are planned to evaluate absorption behavior during exposure of hydrated FGD-wastes to a gas blend containing H₂S, CO₂, and CH₄.

EXPERIMENTAL.

Absorption Reactor. A schematic of one configuration of the reactor used to measure CO₂ absorption for the hydrated samples is shown in Figure 1 (shown with 9" X 1/4"-i.d. tube reactors). This is essentially the reactor described in earlier adsorption/cracking studies of liquid hydrocarbons³ with some modification. The more significant modifications include the introduction of standard gases containing CO₂/Ar or CO₂/CH₄/Ar via the entry line in which pure Ar was previously metered, plugging of the liquids inlet, use of 4" X 3/8"-i.d. reactors in addition to the 9" X 1/4" reactors (most of the hydrated-sample tests), and placement of the 4" reactors in a vertical alignment to provide a more uniform flow of gases through the hydrated samples. Essentially the same measurement system was used to measure absorption of CO₂ by the water/sample slurries except that a pair of 250-mL-capacity gas scrubbers were substituted for the ss tube reactors.

Samples. Many of the study samples examined were obtained from commercial utilities that

preferred to remain unidentified. Thus, only cursory descriptions of the samples will be given and some producers will remain anonymous.

A total of 11 samples were examined. A very brief description along with the identification label used in this report is given in Table I. The fly ash utilized as control (L-FA) is a Class F fly ash from a pulverized-coal-combustion (PCC) utility boiler operating on bituminous coal. The fluidized-bed combustion materials (FU-FA/BA and CC-FA/BA) were derived from circulating or entrained flow units operating on high-sulfur bituminous coal. The coarse material (BA-bed ash) was drained from the bed while the finer material (FA) represents cyclone and baghouse catch. These samples differ primarily in particle size and relative proportions of free lime. Two types of dry post-combustion flue-gas material were utilized in the study, a spray-dryer ash from a large industrial boiler in the Midwest, and materials from the Coolside duct-injection technology. The Coolside materials include a sample (CS) from Ohio Edison's 1990 demonstration of the technology at its Edgewater power plant⁴ as well as materials derived from the CONSOL's Coolside pilot plant in Library, PA (PP1-PP4).⁵

Run Conditions and Procedures. All absorption measurements were made at ambient temperature. Nominal gas flows of 100 mL/min (ambient temperature) for the hydrated-solids tests and 150 mL/min for the slurry tests were metered through each reactor. The gas streams were comprised solely of N₂ in the bypass line and a standard-gas blend (either Ar/CO₂/He-7.5/2.5/90.0 vol%; or Ar/CO₂/CH₄-30.4/49.6/20.1 vol%) in the absorbent line. Argon was included as a tracer gas to eliminate measurements problems associated with minor leaks or instrumental drift. Hydrated samples of known water content were obtained by careful blending of distilled water and dry waste. Between 2 and 5 g of the hydrated samples were packed into the absorbent reactor between quartz-wool plugs. The bypass reactor was packed with 6 g of Ottawa sand.

For the slurry absorption experiments, ~5 g of dry sample was added to 200 mL of distilled water in a 250-mL gas scrubber. The slurry was stirred with a magnetic stir bar for the duration of the experiment. Gas concentrations in the combined sample/bypass exit stream were determined with a VG-quadrupole mass spectrometer (QMS). This unit was operated in a selected-ion-monitoring mode in which intensities for m/e 18-H₂O⁺, 20-Ar²⁺, 28-N₂⁺, 40-Ar⁺, 44-CO₂⁺, and 15-CH₃⁺ (for methane) were recorded at approximately 1-second intervals.

For both the hydrated-solids and slurry tests, data collection was initiated with the switching valve in the bypass position, i.e., with the CO₂ stream passing through the bypass reactor. After a minimum of 150 data points were collected (usually 2-4 minutes), the valve was rotated so that the CO₂ stream was switched to the absorbent reactor and the N₂ stream was simultaneously switched to the bypass reactor. After a selected exposure time, the valve was returned to the initial position to reestablish the QMS baseline.

Following data collection, the QMS data were imported to a spreadsheet where the molecular-ion signal for CO₂ (m/e-44) was ratioed to the Ar-ion signal (m/e-40). The curves described by the CO₂/Ar ratio were then numerically integrated over the interval during which CO₂ was routed to the absorbent reactor to determine the fraction of the CO₂ absorbed. The fraction of CO₂ absorbed was calculated to an absolute basis then to SCF of CO₂ absorbed per ton of waste.

Several of the hydrated samples were retained in sealed vials for post-run XRD analysis to investigate changes in mineralogy resulting from CO₂ absorption. Likewise, selected slurry waters were retained in sealed containers for ICP analysis of heavy metals/cations.

RESULTS

A plot of the CO₂/Ar ion-intensity ratios is shown in Figure 2. In this run, the Ar/CO₂ blend (2.5% CO₂) was initially flowed through the sand-packed bypass reactor, switched to the absorbent bed packed with hydrated FU-fly ash at 3 min, returned to the bypass reactor at 53 min, then again to the absorbent reactor 3-min later. This particular plot demonstrates both the rapid kinetics and the extent to which CO₂ was absorbed in the 9" reactor as well as provides an indication of the reproducibility of the QMS response during the two bypass- and expose-mode intervals. A more complete run, also conducted in the 9" reactor with 2.5% CO₂, is shown in Figure 3. This latter plot demonstrates how the QMS response collected as the CO₂ passes through the bypass reactor (before and after the valve switch) provides a suitable baseline for integration of the ion intensities recorded during passage of CO₂ through the absorbent bed.

Absorption by hydrated solids. Absorption of CO₂ is shown in Figure 4 as a function of water content. These plots were prepared from runs in which 2-5 g (dry basis) of hydrated sample were exposed to flowing CO₂ (49.6%; ~100 mL/min) in the 4" X 3/8"-i.d. reactors. In dry form, none of the wastes examined showed a strong affinity for CO₂. However, with addition of H₂O, the absorption capacity increased rapidly until the water content was sufficiently high to create a mud-like texture in the waste samples. At the highest moisture levels, absorption capacities declined, presumably limited by sample permeability. Maximum absorption ranged from ~1,700 SCF/ton for the FU-FA to ~300 SCF/ton for the control fly-ash sample (L-FA). Limited testing in the 9" reactor showed absorption in excess of 2,000 SCF/ton for the FU-FA sample.

Absorption by water/waste slurries. For the final phase of the study, the ss tube reactors were replaced with a pair of 250-mL gas bubbler/scrubbers. As described earlier, ~5 g of solid waste were added to 200 mL of distilled water in the absorbent scrubber (bypass scrubber contained 200 mL of distilled water). The gas blend containing CO₂, Ar, and CH₄ (~50:30:20) was bubbled through the water in the bypass reactor during the initial bypass interval then switched to the absorbent slurry for up to one hour before returning to bypass. The QMS data collected during the slurry tests was processed the same as those collected during the hydration studies.

Results from the slurry tests are shown in Figure 5. Absorption ranged from less than 1,000 SCF/ton for the L-FA control sample to more than 3,500 SCF/ton for the FU-FA and PP4 samples. These results generally correlate with the free lime data in Table I with the exception of the two samples of bed ash. The significantly larger particle size of the bed ash samples likely limits diffusion of CO₂ into the particle and explains their lower than expected absorption capacity.

Although removal of CO₂ was greater in the slurry tests on an absolute basis, neither the rate or level of maximum absorption was as great as measured for the equivalent hydrated samples. Slurry runs typically required 10-20 minutes before CO₂ response returned to 95% of the original level. Further, at maximum absorption, CO₂ was typically reduced from 49.6% in the feed stream to around 12-15% in the exit stream for the slurry tests as compared to 1% or less in the exit stream for the hydrated-waste tests. However, the shape of the adsorption curves obtained from the slurry tests is thought to be more of a reflection of scrubber design rather than absorption kinetics. It is believed that both kinetics and the maximum level of absorption can be markedly improved with a more efficiently designed bubbler/scrubber (smaller bubbles, longer contact time).

Post-run analysis of hydrated solids and slurry waters. Selected samples from the hydration tests were examined by XRD and compared to similar analyses of unexposed samples. The XRD results indicate that the only significant change in mineralogy following absorption was an increase in calcium carbonate (CaCO₃). There was also a minor increase in ettringite, a hydrous calcium sulfaluminate phase that can substitute carbonate for sulfate in its structure. However, since the samples remained moisturized following exposure (i.e., they may continue to react), it is possible that these minor changes occurred after the absorption run and before the XRD analysis. Regardless, it appears that the CO₂ reacts primarily with available Ca (CaO or Ca(OH)₂) to form carbonate.

Two of the water samples retained from the slurry tests were analyzed for metal/cations content (Table II). Elemental concentrations are in large part controlled by pH which was >12 for these samples. At such high pH, most transition metals are relatively insoluble. This likely explains why none of the elements tested were detected at levels sufficient to suggest unreasonable disposal problems due to the leaching of toxic elements from the waste samples into the slurry water.

SUMMARY

The results obtained in this study clearly show that when hydrated, FGD wastes exhibit a high affinity for CO₂, ranging as high as 3,600 SCF/ton. Further, there are significant differences in the capacity of FGD wastes generated in different plants to absorb CO₂. With the exception of the larger particle-size bed-ash samples, these differences appear to be controlled by the available lime content of a given waste. This is supported by the free-lime data in Table I and XRD analysis which indicated that the absorbed CO₂ reacts with free lime to form CaCO₃. Thus, dry wastes from less efficient utility scrubbers should produce higher-capacity CO₂ absorbents. Finally, analysis of the slurry waters suggests that process waters that may be used in a liquid scrubber can be safely disposed following contact with FGD wastes.

ACKNOWLEDGEMENT

The authors would like to thank K. Saur and B. Schram of the UK-CAER and K. Baker of Jefferson Gas Transmission for their assistance with this project.

REFERENCES.

1. *Coal Combustion Byproduct (CCB); Production & use: 1966-1993. Report for Coal Burning Utilities in the United States.* American Coal Ash Association, 1995, Alexandria, VA, 68p.
2. Personal communications with William Johnson and associates at NIPER in Bartlesville OK and Tom Cooley with Grace Membrane Systems, Houston, TX.
3. Taulbee, D. N., *Prepr., ACS Div. of Fuel Chem., 1993, 38, #1*, American Chemistry Society, Washington, DC, 324-329.
4. Kanary, D.A., R.M. Stanick, H. Yoon, et.al., 1990, Coolside Process Demonstration at the Ohio Edison Company Edgewater Plant Unit 4-Boiler 13. *Proceedings, 1990 SO₂ Control Symposium 3*, EPRI/U.S. EPA, Session 7A., New Orleans, LA, 19p.
5. Withum, J.A., W.A. Rosenhoover and H. Yoon, 1988 *Proceedings, 5th Pittsburgh Coal Conf.* University of Pittsburgh, 84-96.

Table I. Waste samples examined.

Sample#	Label	FGD Waste	Free CaO (wt%)	Source/Comment
1	L-FA	N	2.7	Utility-boiler fly ash
2	FU-FA	Y	19.5	Fluidized bed-cyclone/baghouse catch
3	FU-BA	Y	26.8	Fluidized bed-bed ash
4	SD	Y	5.8	Utility spray dryer
5	CC-FA	Y	8.6	Fluidized bed-cyclone/baghouse catch
6	CC-BA	Y	21.2	Fluidized bed-bed ash
7	PP1	Y	12.9	Coolside pilot plant waste
8	PP2	Y	9.1	Coolside pilot plant waste
9	PP3	Y	8.5	Coolside pilot plant waste
10	PP4	Y	19.9	Coolside pilot plant waste
11	CS	Y	6.5	Coolside demonstration plant waste

Table II. Concentration (ppm) of cation/metals in the waters retained from slurry-absorption tests.

	FU-FA	FU-BA		FU-FA	FU-BA
Ag	<.01	<.01	Mg	87	34
Al	<.05	<.05	Mn	0.013	0.080
As	<.03	<.03	Mo	0.085	0.075
B	5.7	3.9	Na	3.85	0.85
Ba	0.020	0.010	Ni	<.005	0.017
Ca	558	565	P	<.05	<.05
Cd	0.001	0.001	Pb	<.01	<.01
Co	<.005	<.005	Se	<.03	<.03
Cr	<.005	<.005	Si	23	42
Cu	<.005	<.005	Tl	0.013	0.013
Fe	0.015	0.013	V	0.071	0.038
K	3.50	0.45	Zn	0.012	<.002

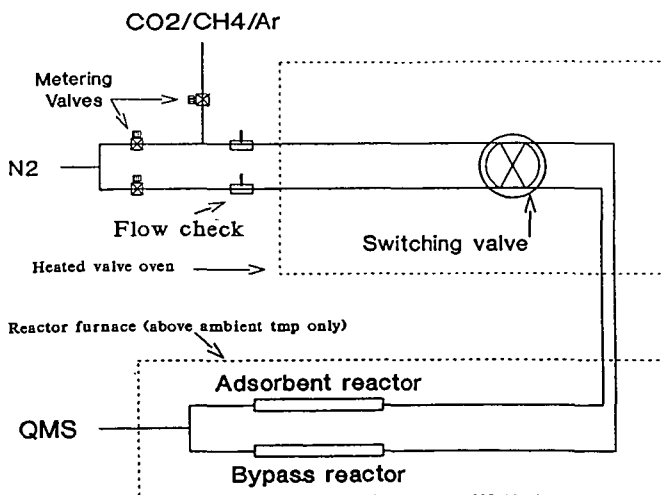


Figure 1. Schematic of the absorption reactor used for the hydrated samples.

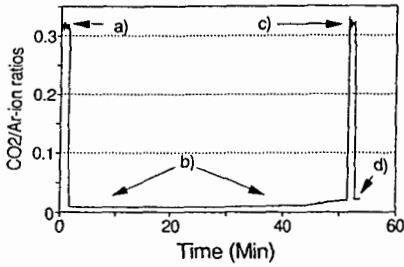


Figure 2. CO₂/Ar ion-ratio curve showing CO₂/Ar ratios as gas blend is routed through a) bypass reactor, b) absorbent reactor, c) return to bypass reactor, and d) return to absorbent reactor.

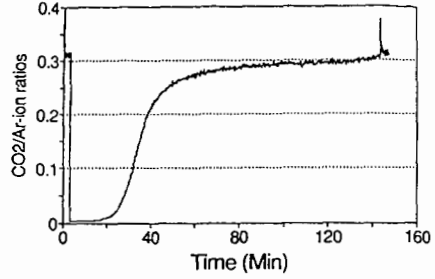


Figure 3. CO₂/Ar ion-ratios during run with FU-fly ash in 9" reactors (1.5 g dry FU-FA; 0.58 g H₂O; 2.5 mL/min CO₂).

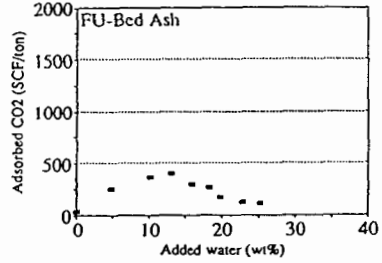
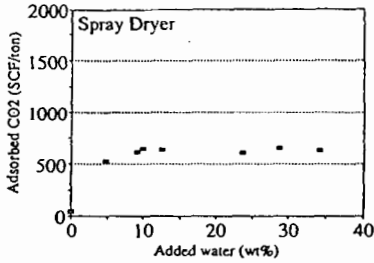
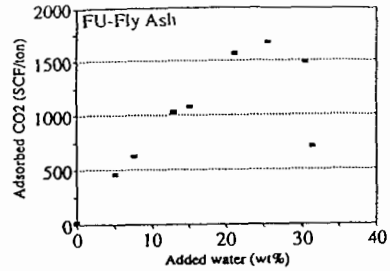
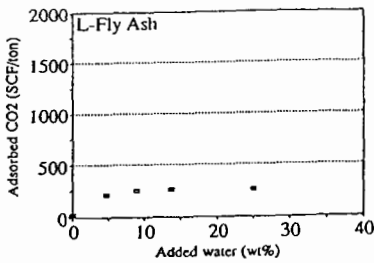


Figure 4. Adsorption of CO₂ by hydrated wastes as a function of water content.

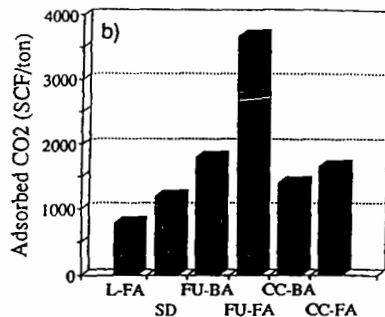
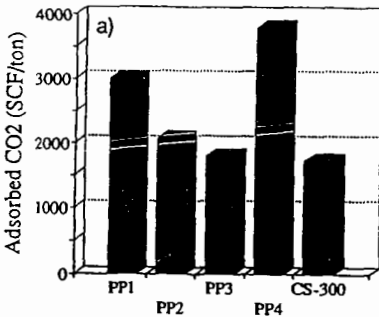


Figure 5. CO₂ absorption by water/waste slurries. a) Coolside wastes; b) all others.

TECHNOLOGIES OF COAL FLY ASH PROCESSING INTO METALLURGICAL AND SILICATE CHEMICAL PRODUCTS

Solomon Shcherban, Int. Assn. of Science, Inc., 110 Bennett Ave., 3H
New York, NY 10033; Victor Raizman, Assn. of Engineers & Science, New York;
Iliya Pevzner, Corall Co. of St.Petersburg Engineer Academy, St.Petersburg

Keywords: coal fly ash, recovery of metals and silica, utilization

ABSTRACT

A study and industrial testing have made for the recovery of aluminum, iron and silica from coal ash, produced by utilities. Alkaline technologies for coal fly ash processing were developed that made it possible to separate the main components of fly ash (SiO_2 , Al_2O_3 , Fe_2O_3) and utilize them separately, producing a large variety of useful products. Some of these technologies have already been successfully tested in pilot programs.

INTRODUCTION

The problem of effective utilization of solid waste from coal-fired power plants is of great importance to many countries. The coal burning utilities of the former Soviet Union generate more than 100 million tons of solid combustion by-products each year. Approximately 1 billion tons of solid waste from utilities is placed in storage and disposal areas. The combustion of coal by utilities in the United States results in the production of over 80 million tons of solid by-products each year yet less than a quarter of coal ash is presently being utilized [1].

The various fields of fly ash application are known [1-3]. In the former Soviet Union much attention has been given to the area of research that is called 'High Technology Ash Application' in the United States [1]. This research focuses on the development of technologies for ash processing with recovery of valuable minerals and metals in particular for the recovery of aluminum. The necessity of this research is caused by the need to find new ways for the utilization of fly and bottom ash and simultaneously to solve the problem of expanding the source of raw materials used in aluminum industry.

Ash contains approximately 1.5-2 times less aluminum oxide than common aluminum raw materials (20-35% Al_2O_3 in ash as compared to 50-62% Al_2O_3 in bauxite). The high level of silica in ashes (40-65% SiO_2) makes it impossible to process them by the easiest and the most economical Bayer method and by the other methods of direct alkaline alumina extraction. Therefore for ash processing other methods are studied: acid, thermal, thermal reducing, electrothermal melting, new alkaline methods.

This paper is dedicated to the development of alkaline methods of ash processing. The laboratory research of alkaline methods of fly ash processing have been done at the Problem Laboratory of Recovery of Light and Rare Metals (Kazakh Polytechnical University, Alma-Ata). Large-scale testing of the alkaline technologies has been conducted at the pilot plants of the All-Union Aluminum-Magnesium Institute (VAMI, St.Petersburg), State Research and Designed Cement Institute (GIPROcement, St.Peterburg), and the Institute of General and Inorganic Chemistry (Erevan).

EXPERIMENTAL

Chemical and Mineralogical Description of Ash Samples

Chemical analysis of typical fly ash derived from Ekibastuz coal are given in Table 1.

Table 1
CHEMICAL ANALYSIS (Wt.%) OF FLY ASH

Power Plant	C o n s t i t u e n t									
	SiO_2	Al_2O_3	Fe_2O_3	Ti O_2	CaO	MgO	Na_2O	K_2O	LOI	Total
Pavlodar	59.82	27.79	5.48	1.65	1.20	0.72	0.40	0.62	4.50	97.68
Ermak	60.50	27.20	5.05	1.90	1.60	0.58	0.30	0.60	4.00	97.73
Troitsk	58.48	30.21	4.78	1.95	1.12	0.66	0.30	0.55	0.80	98.05

The major constituents of the Ekibastuz ashes are silicon dioxide, aluminum oxide and iron oxide which represent about 90-94% of the total. Ekibastuz fly ash is characterized by low content of Na_2O and K_2O ($\leq 1\%$) and CaO and MgO (1.78-2.2).

The mineral part of Ekibastuz coal is represented by kaolinite (60-68%), quartz (27-30%), sider-

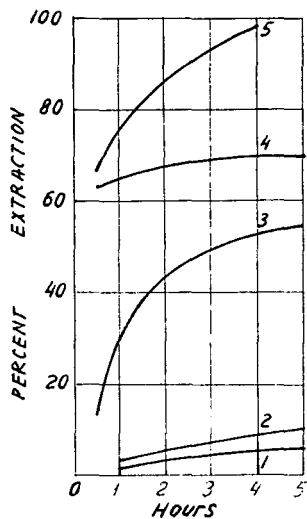


Figure 1. Interaction between alkaline solution and ash compounds: 1 - mullite; 2 - quartz; 3 - ash glassy phase; 4 - ash cristobalite; 5 - synthesized cristobalite.

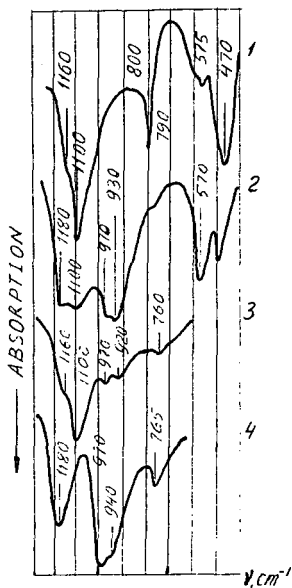


Figure 2. Infra-red Spectra: 1 - ash; 2 - its residue; 3 - ash calcinated at 1250°C; 4 - its residue.

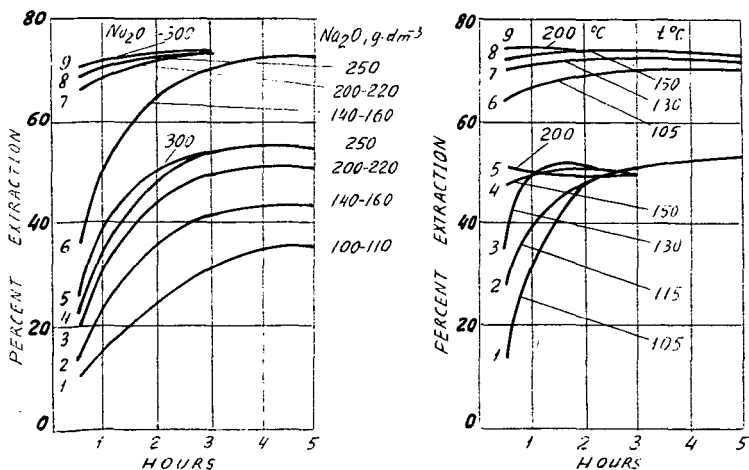


Figure 3. Silica extraction from Fly Ash

crystalobalite maxima $d, \text{\AA}$: 4.09-4.10; 4.52; 3.51 which is well coordinated with the data of crystalobalite alkaline dissolubility (Figure 1). The aforementioned data of chemical, XRD, and IR-spectroscopy research shows that uncombined (free) ash silica is extracted from ash by the alkaline solution.

Hydroalkaline Recovery of Silica from Fly Ash

The influence of various factors on the percentage of silica extraction from fly ash is shown in Figure 3.

The data in Figure 3 shows that free silica is extracted from ash at low rates (temperature 105°C for a duration of 3-4 hours). The process can be realized at atmospheric pressure. The essential augmentation of silica recovery has been reached by means of ash activation which increased the efficiency of silica extraction by 12-20% (Figure 3, curves 6-9).

The intermediates after ash hydroalkaline treatment were the silica alkaline solution (SAS) and the solid residue enriched by aluminum oxide (concentrate of alumina). Chemical composition of SAS, g dm^{-3} : $\text{Na}_2\text{O}=160-220$; $\text{SiO}_2=100-250$; $\text{Al}_2\text{O}_3=2-7$; $\text{Fe}_2\text{O}_3=0.1-0.9$. Concentrate of alumina included %: 44-55 Al_2O_3 ; 30-27 SiO_2 ; 5.5-10 Fe_2O_3 .

Recovery of Iron from Fly Ash by Magnetic Separation

In a number of studies, magnetic separation was applied as a pre-stage before the main operations of ash treatment [6]. Ekibastuz ash consists of 4-10% Fe (as Fe_2O_3). The possibility of recovering the magnetic fraction from Ekibastuz ash and its classified fractions was shown in [7]. The magnetic fractions after raw ash magnetic separation were rich in Fe (60-62% as Fe_2O_3). Classified fractions contained 57.6-66.4% Fe as Fe_2O_3 . Output of the magnetic fractions was 2.12-5%. The non-magnetic residues were depleted of Fe and contained 2.6-3.6% Fe as Fe_2O_3 .

Technology of Alkaline Fly Ash Processing. The Principle Process Flow Sheet

The described findings of hydroalkaline recovery of silica were taken as a basis for the design of the process flow sheet of fly ash processing into metallurgical, silicate chemical products and building materials. The principle flow sheet (Figure 4) includes the hydroalkaline silica extraction from fly ash. This operation allows one to extract the good part of ash silica (60-77%) into the alkaline solution and then to process it into various silicate chemical products (sodium and calcium metasilicates, sodium-silicate mixtures, amorphous and crystalline silica and others). The solid intermediates from ash extraction-alumina concentrate-can be processed into alumina, aluminum, and aluminates by thermal or hydrochemical alkaline methods or can be used for aluminum-silicon alloys, refractories, and concrete production. Mud of the alumina production is a valuable raw material for cements.

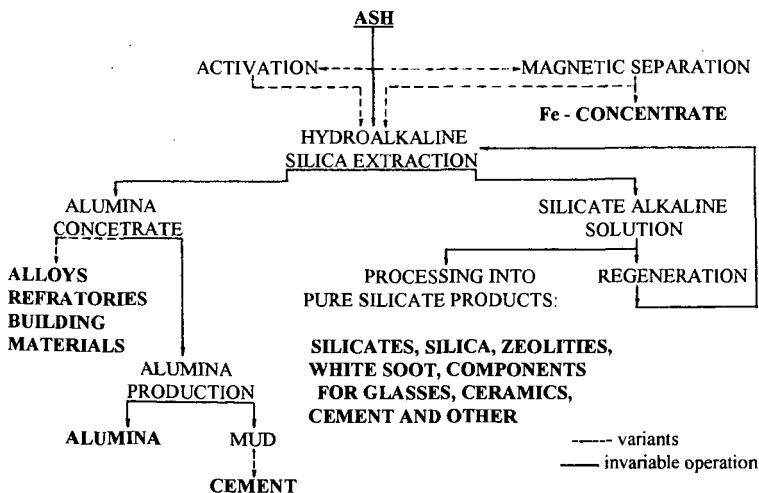


Figure 4. Flow sheet for alumina, silica and iron recovery from ash

Large-Scale Testing of the Alkaline Technologies

Practically all of the main technological operations of the fly ash processing have been tested in pilot programs: ash activation, hydroalkaline silica extraction, settling and filtration of ash pulp, washing of the alumina concentrate, processing it into alumina, producing of portland cement from mud, silica alkaline solutions processing into sodium and calcium metasilicates. Alumina output was made up of 86% Al_2O_3 (90-91.7% at the standard leaching).

REFERENCES

1. Golden D.M. 'Research to Develop Coal Ash Uses.' Ninth International Ash Use Symposium. Proceedings. Orlando, Florida, January 22-25, 1991.
2. Shpirt M.Y. 'Nonwaste Technology: Utilization of Waste from Mining and Processing of Solid Combustible Fossils. Moscow: Entrails' 1986.
3. 'The Combined utilization of Coal Ash of the SSSR in the National Economy', Abstracts, Meeting, Irkutsk, Russia, 11-13 July, 1989.
4. Shcherban S.A., Nurmagambetova S.Kh. 'The Combined Utilization of Coal Ash of the SSSR in the National Economy', Abstract, Meeting, Irkutsk, Russia, 11-13 July, 1989, p.91
5. Suliaieva N.G., Shcherban S.A., Tazhibaeva S.Kh, Romanov L.G. 'Combined Using of Mineral Raw Materials' Periodical. 1982, #3, pp.62-66, Alma-Ata (Russian)
6. Hemmings R.T., Berry E.E. and Golden D.M. 'Direct Acid Leaching of Fly Ash: Recovery of Metals and the Use of Residues as Fullers'. Eight International Coal Ash Utilization Symposium, Washington D.C., October 29-31, 1987, p.38-A
7. Shcherban S.A., Sadykov Zh.S., Pustovalova L.S., Ergaliev G.B., Fridman S.E. 'Ekibstuz Ash Processing into Alumina with Iron Concentrate Production'. Combined Using of Mineral Raw Materials. Periodical, 1985, N4, pp.68-71, Alma-Ata (Russian)

CHARACTERIZATION OF PYROLYSIS OILS OBTAINED FROM NON-CONVENTIONAL SOURCES

J. Houde Jr., J.-P. Charland, Energy Research Laboratories, CANMET, Natural Resources Canada, 555 Booth St., Ottawa, Ont., Canada, K1A 0G1. E-mail: jean.houde@x400.emr.ca

Keywords: pyrolysis oil, automobile shredder residue, pulp and paper sludges

INTRODUCTION

The effluents of pulp bleaching are the main problem of wastewater disposal faced by the pulp industry because of their non-biodegradability. Today the demand for quality discharges requires better methods than conventional biological processes. The changes recently proposed to the federal regulations for controlling discharges from pulp and paper industry operations in Canada have required many operations to install secondary biological effluent treatment process. Such treatment often produce sludges that must be removed from the system and disposed of routinely, usually daily or weekly. At present, Ontario and Québec have the strictest solids disposal regulations in Canada, with leachate criteria that approximate the U.S. Environmental Protection Agency (EPA) toxicity characteristic leaching procedure (TCLP) standard [1]. Most pulp and paper mills in the U.S. have some form of biological treatment, the majority having their own treatment plants, but some are tied into publicly owned treatment plants. Of those which have their own treatment plants, two thirds have aerated stabilization basins and one third have activated sludge [2].

Industrial wastewater secondary treatment using activated sludge techniques has gained increased acceptance in the paper industry. The advantages of activated sludge treatment over conventional aerated lagoons are less real estate requirement, less odour emissions, lower capital cost and higher sludge treatment efficiency [3]. One of the main disadvantages is the production of a large amount of sludge which is difficult to dewater and costly to dispose of. The Canadian pulp and paper industry produces about 2,200 t/d of sludge from wastewater treatment operations. Most of this sludge is produced in wood room or primary clarifiers treating total mill effluents. Approximately 54% of this total is incinerated, with most of the balance being landfilled [4]. Long term environmental uncertainties associated with landfilling, as well as increasing costs and a drive to greater energy efficiency, make it preferable to use the sludge.

When old cars and trucks are sent to scrap yards for shredding to recover ferrous and non-ferrous metals, large quantities of non-metallic waste, referred to as autofluff, are generated. Autofluff is a lightweight mixture of plastics, textile, glass, rubber, foam, paper and rust. Also, this material is contaminated with oils, lubricants and other fluids used in automobiles. The trend to substitute lightweight materials for iron and steel reduces the proportion of recycled metals and increases the amount of waste produced [5-8]. The economics of the shredding industry relates to the recovery and resale of the ferrous metal which is used to produce high quality steel. Over the years, the use of ferrous metals in automobiles has declined whereas that of plastics and non-ferrous metals has increased. There is a clear economic and environmental advantage to salvaging cars, since metals can be utilized that would otherwise end up as trash. In 1992, in Canada, one million cars and trucks were sent to scrap yards, while in the U.S., 11 million vehicles were taken off the road [7]. Autofluff production is estimated at 1,800,000 and 2,860,000 t/a, respectively for Canada and the U.S., most of which ends up in landfill sites.

Of the various disposal alternatives, conversion of these materials by pyrolysis or other proven technology to possible value-added products would reduce the use of costly landfill sites for disposal and utilize this potentially valuable resource. The Wastewater Technology Centre (WTC) of Environment Canada has been developing one such technology since 1982. The thermoconversion process involves low temperature treatment of materials such as sludge from the pulp and paper industry or autofluff, to produce liquid and solid fuel products. A key technical feature of this conversion is the formation of a byproduct oil referred to as pulp and paper sludge derived oil (PPSDO) or autofluff oil. The thermal conversion process has been extensively described elsewhere [9-11].

In 1992, Enersludge Inc., WTC and CANMET's Energy Research Laboratory (ERL) of Natural Resources Canada undertook a joint R&D program. ERL investigated pyrolysis oils obtained from autofluff and pulp and paper mill sludges. Analytical results are presented as well as a comparison of these oils with those obtained from tires and municipal sewage sludge.

EXPERIMENTAL

A set of samples was received for each pyrolysis experiment (PPSDO and autofluff oils). The first samples received included compounds with boiling points up to 150°C (-150°C) whereas the second samples contained compounds boiling above 150°C (+150°C). The +150°C samples

were further distilled to yield three additional fractions each. Fractionation was performed using automated ASTM D-1160 short path distillation apparatus. Fraction cuts were selected to reflect conventional cut points from the petroleum industry:

- ▶ 150°C-350°C - typical cut point for middle distillates
- ▶ 350°C-525°C - typical cut point for heavy gas oils
- ▶ +525°C - usual distillate-residue cut point

Physical and chemical analyses were performed according to appropriate ASTM methods.

The ¹H, DEPT ¹³C and ¹³C data were acquired on a VARIAN XL300 operated at 300 MHz in the ¹H mode and 75 MHz in the ¹³C mode. The pulse sequence in DEPT experiments transfers the polarization of the hydrogen to the carbon nucleus to selectively increase its signal. The polarization transfer effect is dependent on the number of hydrogens bonded to a given carbon nucleus. This technique is used to distinguish between primary, secondary, tertiary and quaternary carbon atoms. The NMR spectra are presented in Fig. 1.

Infrared spectra were obtained using a PC-driven BOMEM MB100 Fourier transform infrared (FTIR) spectrometer fitted with a standard sample mounting device. The IR spectra from liquids were collected using a liquid cell fitted with a 13-mm diam circular window. The liquid cell windows are made of KBr and are separated by 0.02 mm. The spectra of the 350°C-525°C colloidal fractions were collected using the smearing technique on conventional 13-mm circular KBr discs. The IR spectra are presented in Fig. 2.

GC/MS work was performed on a Hewlett Packard 5890 GC coupled to a medium resolution mass spectrometer (MS). Chromatographic separation of the sample was done using a Hewlett Packard HP-1 30 m long methyl-silicon bonded fused silica capillary column of medium resolution fitted on the GC. This column is used for separating molecular components in a mixture based on their boiling point. The samples were injected in the GC at 35°C then heated to 200°C at 5°C/min. The temperature was maintained for 10 min at the end of the temperature profile. The chromatographed compounds were identified through a MS data library search.

RESULTS AND DISCUSSION

The +150°C liquids resembled light molasses, similar to a vacuum tower gas oil from a petroleum refinery. The -150°C materials were brown liquids. All samples had an odour characteristic of burnt organic matter. The lower boiling products had the strongest odour. The -150°C oils and the 150°C-350°C fractions were characterized by IR, ¹H & ¹³C NMR and GC/MS.

Table 1 summarizes the fractionation results for the PPSDO and autoluff samples. For comparison, literature data for a tire oil are also included. With an initial boiling point (IBP) of 155°C, the fractionation of the +150°C autoluff sample yielded 90 wt % of distillate composed of 37 wt % in the middle distillate range and 53 wt % in the heavy gas oil range. This range is similar to that of a typical petroleum sample. The PPSDO +150°C sample had an IBP of 102°C and 76 wt % distillate of which 49 wt % was in the middle distillate range and 27 wt % in the heavy gas oil range. Fractionation of the autoluff sample produced more distillate of a heavier nature than the PPSDO. When compared to tire oil, these oils had higher IBPs because they were condensed at a set temperature whereas the tire oil was not. Therefore we cannot compare the distillate yields further.

During fractionation of the PPSDO +150°C sample, the maximum distillate temperature was 501°C due to the limitation of the pot temperature (400°C) from the automatic apparatus used for the distillation. The material loss was 6.0 wt % due to distillate that was trapped in the column and in the condenser. The trapped distillate was so waxy that heating the condenser to a maximum temperature of 80°C in order to recover some distillate was unsuccessful.

The samples were also analyzed using a series of tests commonly used for fuel analysis. Table 2 shows the results as well as literature data for sludge derived oil (SDO), tire oil, No.2 diesel fuel and No.6 fuel oil. The heat of combustion values for the sludge derived materials namely, PPSDO and SDO, are significantly lower, and their densities at 15°C are higher than the corresponding values for the autoluff oil, tire oil and the two fuels.

Table 2 also gives elemental analysis of the samples. Clearly, PPSDO and SDO produced oils having a lower carbon content. However, their H/C ratios are still comparable to the other data mainly due to their lower hydrogen content. Heteroatom levels, particularly N and O, are very high when compared with the other oils. Pour points of these pyrolysis oils fall in the fuel oil range and are much higher than diesel oils.

Figure 1 shows the proton-decoupled ¹³C NMR spectra of two autoluff and two PPSDO oil fractions. The spectrum of the -150°C autoluff fraction exhibited a signal at 45 ppm associated with the -CH₂-O- group, an assignment confirmed by ¹³C DEPT NMR (not shown). This

functional group is absent in the -150°C PPSDO fraction. The spectrum of the -150°C PPSDO fraction shows a signal at 182 ppm assigned to -COOH carbons. No carbonyl signal was observed in the C=O region of the -150°C autofluff fraction spectrum.

A comparison of the NMR spectra of the high boiling point fractions in Fig. 1 revealed significant differences. The spectrum of the PPSDO fraction shows many signals in the 170-180 ppm region due to various -COO(R,H) carbons. No signal was observed in the -COO- region of the autofluff fraction spectrum. Signals in the 150-160 ppm range on both spectra are due to the oxygen-bonded aromatic carbon in phenols. Signals in the 110-115 ppm region on the autofluff spectrum were assigned to terminal =CH₂'s in olefinic structures by ¹³C DEPT NMR.

Figure 2 shows the infrared spectra of selected autofluff and PPSDO fractions. The PPSDO spectra display absorptions in the 3200-3600 cm⁻¹ region which are more intense than in the autofluff fractions. This intensity also is accompanied by stronger and more complex carbonyl vibration band patterns in the PPSDO's than in the autofluff spectra. This indicates and confirms the presence of carboxylic acids suggested by NMR. Another difference between these two types of oils can be observed in the autofluff fraction spectra which display weak but well resolved olefinic and aromatic =C-H stretching and bending mode bands. This suggests the presence of significantly higher amounts of aromatic and olefinic compounds in the autofluff oil fractions.

Table 3 lists GC/MS derived compound type distributions in the low and high temperature PPSDO and autofluff oil fractions. Table 3 indicates that:

- 1) PPSDO fractions contained carboxylic acids;
- 2) autofluff fractions are more aromatic and olefinic than PPSDO fractions;
- 3) low temperature fractions are more aromatic than high temperature fractions;
- 4) high temperature fractions contain more alcohols than low temperature fractions;
- 5) high temperature PPSDO fraction contains a significant amount of nitriles.

CONCLUSIONS

Our study has shown that pyrolysis oils and their derived fractions are very complex mixtures of compounds including significant proportions of aromatics and olefins as well as nitriles, alcohols and ketones. In addition, carboxylic acids were found in PPSDO. Pyrolysis oil's heat of combustion and density values fall within the normal fuel oil range.

The high content of olefins and aromatics of these oils and their high H/C ratios would suggest possibilities as feedstocks for low cost, large volume surfactant utilization. The surfactants could be produced by sulphonation or sulphation reactions. A large-scale use would be for enhanced oil recovery for both conventional and heavy oil/bituminous sands and for cleaning heavy bunker oil pipelines. Also for PPSDO, polymerization in asphalt could be performed to improve asphalt cement quality for adhesion to aggregates due to its high nitrogen content.

The low sulphur content and the high heating value of the autofluff sample suggest it could be utilized as a liquid fuel, possibly by blending it with fuels of petroleum origin in order to lower the sulphur level. While the autofluff oil cannot be considered as a diesel fuel, it could be considered as a blending agent for use with a No.6 fuel oil. The autofluff characteristics resemble those of the No.6 fuel oil more than those of diesel.

ACKNOWLEDGEMENTS

The authors wish to thank WTC for its financial and technical support and the assistance in interpreting the results of this work. The authors acknowledge the technical assistance and contributions of the staff of the Fuel Quality Assessment Section and Dr. Heather Dettman and Mr. Gary Smiley for providing the NMR and GC/MS spectra, respectively. Federal support of this work was provided through the Federal Program on Energy Research and Development (PERD).

REFERENCES

1. Crawford, G.V., Black, S., Miyamoto, H. and Liver, S., "Equipment selection and disposal of biological sludges from pulp and paper operations", Pulp & Paper Canada 94:4:37-39, April 1993.
2. Springer, A.M. "Bioprocessing of pulp and paper mill effluents - past, present and future", Paperi ja puu paper and timber 75:3:156-161, 1993.
3. Garner, J.W. "Activated sludge treatment gains popularity for improving effluent, Pulp & Paper 64:2:158-163, February 1990.
4. Salib, P. "Evaluation of circulating fluidized bed combustion of pulp and paper mill sludges", Contract report Bioenergy Development Program DSS Contract No.: 23216-8-9056/01SZ, RPC, Fredericton, NB, Canada, October 1991.
5. Day, M. "Auto Shredder Residue - Characterization of a solid waste problem", NRCC Special Report EC123992S, NRC Institute for Environmental Chemistry, 1992.

6. Voyer, R. "Étude technico-économique et environnementale des procédés de traitement de résidus des carcasses d'automobiles", CRIQ Report VPOIT-91-098, Centre de recherche industrielle du Québec, 1992.
7. Pritchard, T. "The over 75% solution", Globe and Mail Report on Business, December 1992 issue.
8. Braslaw, J., Melotik, D.J., Gealer, R.L. and Wingfield, Jr, R.C. "Hydrocarbon generation during the inert gas pyrolysis of automobile shredder waste", Thermochemica Acta 186:1:1-18, 1991.
9. Martinoli, D.A. "Converting sewage sludge into liquid hydrocarbon - the OFS process", Hydrocarbon Residues and Waste: Conversion and Utilization Seminar, Edmonton, Alberta, Canada, September 4-5, 1991.
10. Campbell, H.W. and Bridle, T.R. "Sludge management by thermal conversion to fuels", Proc. New Directions and Research in Waste Treatment and Residuals Management, Vancouver, 1985.
11. Campbell, H.W. and Martinoli, D.A. "A status report on Environment Canada's oil from sludge technology", Proc. Status of Municipal Sludge Management for the 1990s, WPCF Specialty Conference, New Orleans, 1990.
12. Mirmiran, S., Ph.D. Thesis, Department of Chemical Engineering, Université Laval, Québec, Canada, 1994.
13. Kriz J.F. et al. "Characterization of sludge derived oil and evaluation of utilization options", Division Report ERL 90-50 (CF), November 1990.
14. Kirk-Othmer Encyclopedia of Chemical Technology, 3rd Edition, vol. 11, John Wiley & Sons, p. 357.
15. Personal communication, September 1993.

Table 1 - D-1160 fractionation results of pyrolysis oil samples.

Fraction	PPSDO	Autofluff	Tire oil ¹
IBP (°C)	102	155	37
IBP-350°C (wt %)	49	37	56
350°C-525°C ² (wt %)	27	53	37
Total (IBP-525°C) (wt %)	76	90	93
Residue (+525°C) (wt %)	18	8	7
Loss (wt %)	6 ³	2	n/a ⁴
Water (wt %)	trace	0	n/a

Table 2 - Physical and chemical analysis data of pyrolysis oil samples and petroleum fuels.

Analysis	PPSDO	Autofluff	SDO ⁵	Tire oil ²	No.2 Diesel	No.6 Fuel oil ⁶
Calorific value (MJ/kg)	32.1	41.8	35.3	43	44.9	42.3
(1000 btu/lb)	13.8	18.0	15.2	18.5	19.3	18.2
Density @ 15°C (kg/m ³)	1073.2	931.1	<1002	n/a	864.1	980
Elemental analysis (%)						
Carbon	68.1	83.3	72.4	85.9	86.9	85.7
Hydrogen	8.99	11.4	9.88	10.6	12.4	10.5
Nitrogen	8.82	1.50	6.35	1.4	n/a	2.0
Oxygen	12.6	3.2	10.8	1.2	n/a	n/a
Sulphur	0.39	0.5	1.11	0.9	0.44	0.5-3.5
H/C ratio	1.6	1.6	1.6	1.5	1.7	1.5
Pour point (°C)	6	>24 ⁷	0	-6	-40	0

¹ Data from reference [12]

² End-point for distillation of PPSDO: 501°C and for tire oil: 469°C

³ Large loss due to distillate trapped in column and condenser

⁴ n/a: not available

⁵ Data from reference [13]

⁶ Data from references [14-15]

⁷ Film formed on top preventing pouring of sample. Thus the pour point was reported as >24°C.

Table 3 - Compound type distribution in selected pyrolysis oil fractions by GC/MS.

Compound type	-150°C		102-350°C		150-350°C	
	PPSDO	AUTOFLUFF	PPSDO	AUTOFLUFF	PPSDO	AUTOFLUFF
Alcohols	8.8	10.8	14.7	12.6		
Aldehydes		3.7	0.5	1.3		
Amines	2.4		3.2	0.9		
Amides	3.1		2.7	1.1		
Aromatics	10.2	48.7	5.2	18.2		
Carboxylic acids	27.8		6.0			
Epoxides					0.6	
Esters		0.5	0.2	0.4		
Ethers	0.8		1.2	0.5		
Heterocyclics	5.7		7.1	2.3		
Ketones	2.8	6.8	4.4	5.1		
Nitriles	1.6	5.0	17.4	2.2		
Nitro			0.1			
Olefins	11.7	14.9	6.6	24.0		
Paraffins	14.6	9.7	8.9	29.5		
Total	89.5	100.1	78.2	98.7		

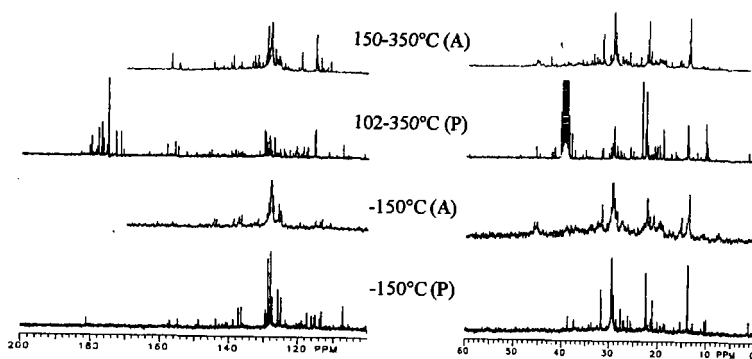


Fig. 1 - ^{13}C NMR regions (0-60 and 100-200 ppm) of selected autofluff (A) & PPSDO (P) fractions.

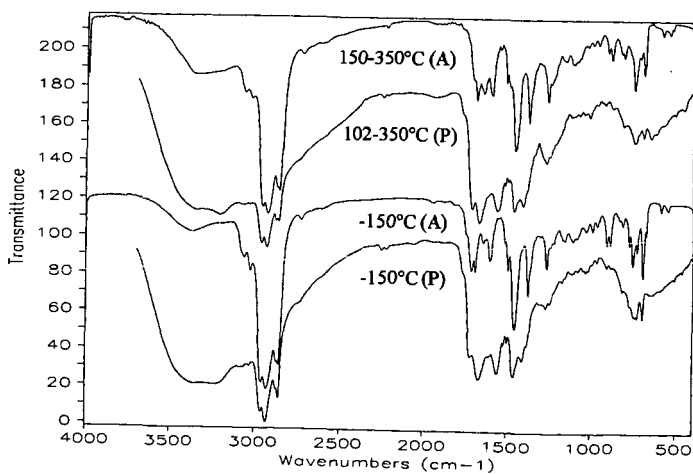


Fig. 2 - IR spectra of selected autofluff (A) & PPSDO (P) fractions

CATALYTIC PYROLYSIS OF AUTOMOBILE SHREDDER RESIDUE

Gregory G. Arzoumanidis, Michael J. McIntosh,
Eric J. Steffensen, Matthew J. McKee, and Timothy Donahugh
Energy Systems Division, Building 362
Argonne National Laboratory
Argonne, Illinois 60439

Keywords: Catalytic Pyrolysis, Plastics, Automobile Recycling

INTRODUCTION

In the United States, approximately 10 million automobiles are scrapped and shredded each year. The mixture of plastics and other materials remaining after recovery of the metals is known as Automobile Shredder Residue (ASR). In 1994, about 3.5 million tons of ASR was produced and disposed of in landfills. However, environmental, legislative, and economic considerations are forcing the industry to search for recycling or other alternatives to disposal (1,2).

Numerous studies have been done relating the ASR disposal problem to possible recycling treatments such as pyrolysis, gasification, co-liquefaction of ASR with coal, chemical recovery of plastics from ASR (3), catalytic pyrolysis (4), reclamation in molten salts (5), and vacuum pyrolysis (6). These and other possibilities have been studied intensively, and entire symposia have been devoted to the problem (3). Product mix, yields, toxicology issues, and projected economics of conceptual plant designs based on experimental results are among the key elements of past studies. Because the kinds of recycling methods that may be developed, along with their ultimate economic value, depend on a very large number of variables, these studies have been open-ended. It is hoped that it may be useful to explore some of these previously studied areas from fresh perspectives. One such approach, currently under development at Argonne National Laboratory, is the catalytic pyrolysis of ASR.

EXPERIMENTAL METHOD

To eliminate variability due to nonuniform sampling, testing was begun using a "synthetic ASR" made up from pure materials on the basis of a best estimate of the inert-free ASR composition (Table 1). For the catalytic studies, pyrolysis occurs in a ceramic tube reactor inserted into the 30-cm heating zone of an electric furnace. The ASR is positioned in the reactor by means of an inconel sample holder. Time/temperature profile is controlled by microprocessor. The majority of experiments are conducted using the profile shown in Figure 1. Faster rates of pyrolysis correspond to the profile in Figure 2.

Liquids are collected in a series of three condensers, the first water-cooled, the others cooled by glycol at -20°C. Liquids are analyzed by GC/MS. Product gas samples are collected on-line in steel containers and analyzed by comparison with GC standards, using a 25-m X 0.53-mm fused silica column coated by Poraplot U, available from Chrompack. The gas mixtures are further analyzed by FTIR.

For kinetic studies, a smaller tube and a furnace with a 15-cm heating zone are used. The ASR sample is usually 10 gm. The reactor weight is continuously monitored by a sensitive transducer. The weight increase of a condenser is monitored by a second transducer. The time/temperature profile inside the reactor can be more accurately controlled in this smaller system. The profile, giving the results presented below, was ramped from ambient to 700°C in 60 min and maintained at 700°C for 100 min. With this equipment, a continuous time/mass profile is obtained of the reactor residue, liquids condensed, and gases produced.

RESULTS

Catalytic pyrolysis of synthetic ASR was conducted in the presence of several oxides, montmorillonite, and ASR char (Table 2). The amount of gases produced (determined by difference) varied within a rather narrow range. The amount of CO₂ in the sample was determined by using an ascarite-filled trap. The total amount of CO₂ from uncatalyzed reactions is usually 6-9% of the synthetic ASR weight. In one case, 18% CO₂ was obtained, but the pyrolysis was run in the presence of Fe₃O₄, and oxidation of carbon by the metal oxide is likely.

Three gas samples were obtained at three different temperatures during each experiment. The first sample was collected at 400-440°C pyrolysis temperature, the second at 500°C, and the third at 650°C. GC analyses of the first samples gave the distribution of gases shown in Table 3. The relative amounts of each separate gaseous hydrocarbon in the table vary widely, showing the large effect of catalyst on gas yields. Despite this variability, certain trends are clear. Most interesting is the large amount of CH₃Cl formed in the first sample, in one case as high as 90% of the gases. Because a preliminary survey of the pyrolysis literature yielded no reports of this phenomenon, we proceeded with caution despite positive GC and FTIR identification of CH₃Cl. Accordingly, experiments were conducted on synthetic ASR, with its only chlorine-containing

material, PVC, removed. These tests produced essentially no CH_3Cl . In these experiments, CH_4 in the first gas sample was at its highest level (23%). It was also found that addition of Na_2CO_3 to the pyrolysis reaction reduces CH_3Cl formation and increases the level of CH_4 in the first stage. Given these results, the information in Table 3 offers several clues concerning the mechanism and kinetics of ASR pyrolysis. These are discussed below. Interestingly, the relative amounts of the pyrolysis gases from the second (500°C) and third (650°C) samples do not change appreciably, as indicated in Table 4. Changes in the relative amounts of the gases during the duration of the pyrolysis are estimated in Figure 3. This illustrates the large effect of the pyrolysis time/temperature profile on gas product distribution. Several investigators have noticed different product distributions under a variety of experimental conditions (2a). However, a direct effect of the profile is now clearly seen in the figure. This result raises the possibility that the distribution and composition of gaseous and liquid products can be manipulated by variation of the time/temperature profile. This possibility, which could be of economic importance, is now under investigation.

As shown in Table 2, the residual solids (char) yield varied with catalyst type but remained in the range of 23-33% of the initial ASR weight. Lower levels of char yield translate into higher amounts of liquids, possibly an economically desirable effect. A number of binary oxides containing ZnO as one of the catalyst components appear to reduce the formation of char. Other additives (magnesium titanate, zirconate, Fe_3O_4 , montmorillonite) do not yield results very different from the control run without catalyst. The effects of CuO and $\text{TiO}_2\cdot\text{SiO}_2$ also are marginal. In evaluating a commercial ASR recycling process, low cost is of foremost importance. Expensive catalysts, such as the binary oxides of Table 2, are not likely to prove directly useful. The incentive for studying these more expensive materials is to gain an understanding of possible effects, which may aid in the development of cheaper catalysts.

Two classes of liquids are formed by the pyrolysis of ASR. The organic class contains over 50 organic compounds, as analyzed by GC/MS, and the aqueous class contains water and water-soluble oxygenates, primarily acids and alcohols. Water may be physically present in the ASR or may be produced chemically by primary or secondary pyrolysis reactions (see discussion). Chlorine-containing compounds could not be detected by GC/MS in either liquid class. Production of chlorine-free liquid is a desirable feature of a commercial ASR reclamation process if the liquid is to be used as fuel. In this case, it is also desirable to increase the yield of the organic class of liquid. The effects of various catalysts and pyrolysis conditions on maximizing organic liquids are currently under investigation.

DISCUSSION

The pyrolysis of each separate ASR component has been extensively studied by numerous investigators, and mechanisms have been proposed (7). These mechanisms are polymer-structure-dependent and may differ within the same class of polymers. For example, thermal degradation of polyurethanes may occur by three different types of hydrogen transfer: N-H, α -CH, and β -CH, depending on the exact monomeric and polymeric structure of the pyrolyzing material (8). It is generally recognized that pyrolysis in a highly reducing environment proceeds via a radical mechanism. Detailed discussion of these mechanisms is beyond the scope of this paper.

The mechanism of ASR pyrolysis is very complex. Single products (e.g., methane and other aliphatic hydrocarbons) may be formed via different mechanisms, depending on the type and structure of the polymer of origin. Therefore, it is difficult to present a unified mechanism by observation of pyrolysis products alone. An important consideration, however, is the range of different temperatures at which degradation begins for each type of polymer. Polyurethanes may start degrading just above 200°C (7). Removal of HCl from PVC takes place at a relatively low temperature, and it is completed almost before the degradation of the hydrocarbon backbone begins (9). Similar observations may be made for other reactions, such as decarboxylation of nylon, polyesters, polyurethanes and acrylics, formation of chemical water from wood and paper, etc. Thus, it is reasonable to assume that each polymer begins the pyrolysis process individually, based on its own structural and thermodynamic character.

One of the key roles of catalysts is to lower the decomposition temperature by lowering the activation energy for some reactions. A single catalyst will not cause the same decrease of activation energy for all reactions of all ASR components. It is likely the main reason for the wide variation of the relative amounts of products in the first gas sample (Table 3) is the variability of catalyst effects as the temperature reaches a level where the most facile reactions are fairly rapid. However, most of the ASR polymers, after losing such weak-link components as CO_2 , HCl, and H_2O , revert to mostly hydrocarbon backbones, which likely are very similar. This probably is the reason for the limited variations in the product distribution of the second and third gas samples (Table 4).

From the above discussion, at least two distinct stages in the pyrolysis of ASR are hypothesized. The first stage ends at about 300°C, and the second, in our case, continues up to

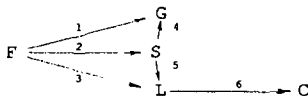
700°C. Preliminary experiments suggest that most of the CO₂, CO, H₂O, CH₃Cl, and possibly some nitrogen-containing components are being released in the first stage. Significantly, these materials carry most of the hetero-atoms that may interfere with the overall quality of useful ASR pyrolysis products.

The formation of CH₃Cl in relatively high concentrations during the first stage offers an indirect view of the reactions occurring during synthetic ASR pyrolysis. It is postulated that HCl released from PVC attacks N-containing polymers, such as polyurethane, to form quaternary cationic nitrogen species; this is followed by scission of the polymer chain through CO₂ elimination, with subsequent formation of an olefinic end-group and an amine, as described earlier (8). The amine, most likely containing an N-CH₃ moiety (8), is further attacked by HCl to form a second, low-MW quaternary salt that decomposes to yield CH₃Cl.

To test the two-stage pyrolysis hypothesis, separate first- and second-stage pyrolysis experiments are under way. The products from each stage are recovered, and the residue from the first pyrolysis stage is used as starting material for the second. Preliminary results indicate that the first residue is about 75% by weight of the synthetic ASR charged. The first-stage liquids are mostly of the aqueous class; about 80-90% of the total CO₂ is released, and more than 90% of the CH₃Cl is released. Only very low levels of gaseous hydrocarbons form during the first stage. Most of the oxygen is removed in the first stage in the form of CO₂, CO, and H₂O, so secondary reactions of these inorganics with the residue are minimized (10). Therefore, second-stage pyrolysis yields primarily organic liquids and a gas rich in olefinic and paraffinic hydrocarbons.

A conceptual, two-stage ASR pyrolysis process that segregates the products from the two stages is envisioned. It could produce commodity methyl chloride in the first stage and valuable feedstock chemicals in the second stage. The potential for producing products from ASR pyrolysis more valuable than liquid fuel may thus be possible.

The above possibilities suggest a need to determine ASR pyrolysis kinetics experimentally. The smaller reactor system described in the experimental section was developed and operated for this purpose. In a universal reaction scheme that seems to fit the kinetic data, six universal reactions and five universal reactants and products in ASR pyrolysis are assumed: fresh ASR (F), gaseous products (G), unvaporized liquids (L), solid residue (S), and condensed liquids (C). The sum of F, L, and S (denoted as R) is retained in the reactor and monitored by the first transducer; C is monitored by the second transducer, and the weight of gases is obtained by difference. The results of an early ASR pyrolysis run are graphically presented in Figure 4. These results are correlated by the following simple scheme of universal reactions:



If reactions 1 through 6 are assumed to be Arrhenius-type first-order reactions, the kinetic model is simple and easily solved. The best-fit Arrhenius constants are given in the figure. The lines in the figure represent the best-fit model, and the points are from the experimental run. These results are consistent with the two-stage ASR pyrolysis hypothesis given above. Universal reactions 1, 2, and 3 with relatively low activation energies dominate the process initially at low temperatures. When higher temperatures are reached, reactions 4 and 5 become significant. Note that reaction 5, the production of liquids from solids, continues throughout the run, as evidenced by the mirror-image slopes of the R and L lines. Results like those presented in Figure 4 are currently being used to evaluate and develop conceptual commercial pyrolysis processes. A more detailed discussion of the kinetic model and its applications will be presented in a later paper.

CONCLUSIONS

The following conclusions, based on early but nevertheless solid experimental data, must be considered tentative, awaiting results from additional confirmatory experiments that are currently under way:

1. Interaction of ASR components during pyrolysis modifies product distributions relative to single-component pyrolysis.
2. It is hypothesized that ASR pyrolysis occurs in two stages. The early, low-temperature stage (300°C) produces mostly inorganic, light gases and high yields of methyl chloride and is susceptible to modification by catalysts. The later, high-temperature stage (700°C) produces mostly organic liquids and gases and is less affected by the catalysts studied so far. Tests to identify catalysts effective in the second stage are under way.
3. Chlorine-containing compounds have not been found in ASR pyrolysis liquids.

4. A universal reaction scheme based on first-order Arrhenius kinetics can be fit to ASR pyrolysis kinetic data and is consistent with the two-stage hypothesis.
5. The two-stage hypothesis increases the possibilities for devising two-stage commercial ASR pyrolysis processes that have improved economic potential.

ACKNOWLEDGMENT

This work was supported by the U.S. Department of Energy, Assistant Secretary for Energy Efficiency and Renewable Energy, under contract W-31-109-Eng-38.

The GC/MS analyses were done by the Analytical Chemistry Laboratory at Argonne National Laboratory.

REFERENCES

1. Automotive Engineering, August 1994, p. 29
- 2a. Day, M., Z. Shen, J.D. Cooney, Proc. Auto Recycle '94, p. 169
- 2b. Agarwar, K., SPE, Proc. "Plastics Recycling: Technology Charts the Course," Schaumburg, Ill., 1994, p. 232
- 2c. Tabery, R.S., Proc. Shredder Operations Conference, Austin, Texas, 1990, p. 1
- 3a. Proc. Auto Recycle '93, Schotland, Southfield, Mich.
- 3b. Proc. Auto Recycle '94, Schotland, Dearborn, Mich.
4. Compton, W.D., N.A. Gjostein, Joint Industry/University Research Programs, DOE Contract No. DE-AC02-78ER10049, May 15, 1984
- 5a. Pierce, A., Proc. Auto Recycle '92, p. 215
- 5b. Chambers, C., J.W. Larsen, W. Li, R. Wiesen, Ind. Eng. Chem. Process Res. Dev., 1984, 23, 648-654
6. Roy, C., P. Mallette, Proc. Energy From Biomass and Wastes, IGT Conference XVI, 1992, p. 827
7. Flynn, J.H., R.E. Florin, "Pyrolysis and GC in Polymer Analysis," S.A. Liebman and E.J. Levy, Eds., Marcel Dekker Inc., New York, p. 149
8. Rumaou, L.P., K.C. Frisch, J. Pol. Sci., Part A-1, 10, 1499-1509 (1972)
9. O'Mara, M.M., J. Pol. Sci., Part A-1, 8, 1887-1899 (1970)

The submitted manuscript has been authored by a contractor of the U.S. Government under contract No. W-31-109-ENG-38. Accordingly, the U.S. Government retains a nonexclusive, royalty-free license to publish or reproduce the published form of this contribution, or allow others to do so, for U.S. Government purposes.

TABLE 1: SYNTHETIC ASR

COMPONENTS	AMOUNT PER RUN (g)
Wood	6.7
33% Glass Reinforced Polyester	3.91
Tar	3.35
Polyurethane Foam	2.23
Polypropylene	1.89
PVC	1.55
ABS	0.78
Nylon	0.44
Acrylic	0.44
TOTAL WEIGHT	21.29

TABLE 2: PYROLYSIS OF "SYNTHETIC" AUTOMOBILE SHREDDER RESIDUE - ASR

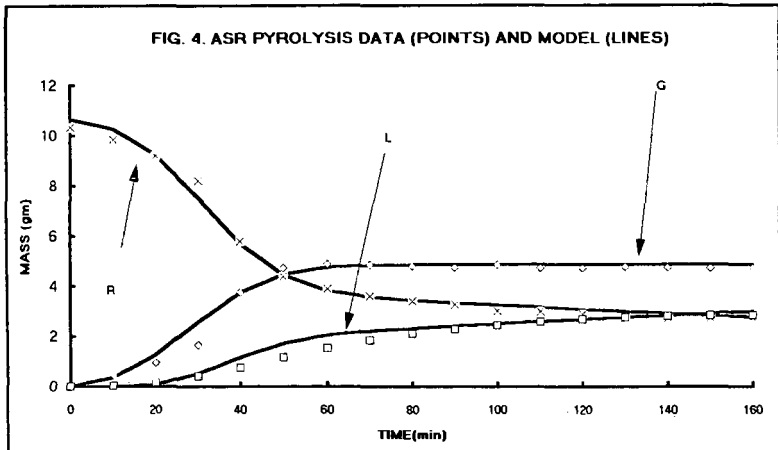
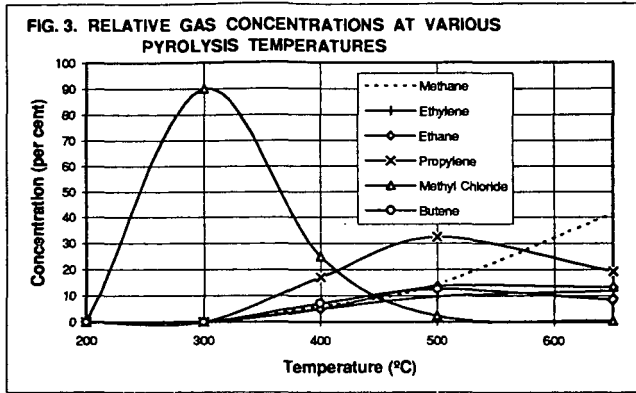
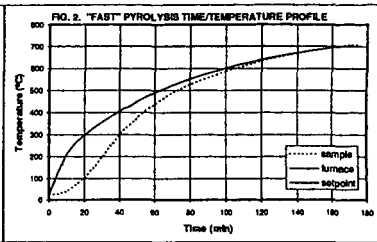
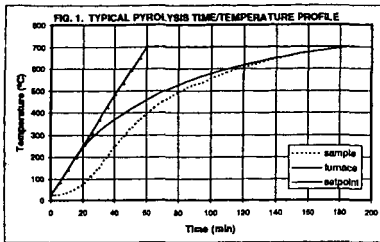
RUN No.	CATALYST	WEIGHT PERCENT OF PYROLYSIS PRODUCTS				
		ORGANIC LIQUIDS	"AQUEOUS" LIQUIDS	CHAR	GAS	CO ₂ MAT. BAL.
1	NONE	8.1	15.3	33.2	43.4	6.2
2	NONE (fast t-ramp)	6.7	15.5	33.1	44.7	8.1
3	NONE (w/o PVC)	6.7	16.1	32.2	45.0	9.1
4	MgO-ZnO	9.5	22.3	24.4	43.8	ND
5	MgO-ZnO	9.7	22.4	23.9	44.0	ND
6	ZnO-TiO ₂	10.2	18.1	27.1	44.6	ND
7	ZnO-TiO ₂	8.9	18.9	23.5	48.7	13.4
8	TiO ₂ -SiO ₂	8.8	18.2	27.2	45.8	ND
9	ZnO-Al ₂ O ₃	9.5	20.0	24.7	45.8	ND
10	MgZrO ₄	7.7	14.2	32.1	46.0	ND
11	MgTiO ₃	8.2	14.4	32.1	45.3	ND
12	Fe ₂ O ₃	9.7	15.3	31.9	43.1	18.2
13	CuO	7.7	16.9	27.5	47.9	11.7
14	Montmorillonite K 10	8.8	17.1	30.4	43.7	6.6
15	ASR Char	7.2	14.9	31.6	46.3	8.9

TABLE 3. COMPOSITION OF GASES (PER CENT) BY GC - FIRST SAMPLE

RUN No.	CATALYST	TEMP. °C	Methane	Ethylene	Ethane	Propylene	Methyl Chloride	Butene	Butadiene	Unknown 1	Unknown 2
1	NONE	400	3.3	1.5	1.5	2.8	87.4	3.0	0.0	0.4	0.0
2	NONE (fast t-ramp)	400	3.6	1.5	1.5	2.8	87.0	2.8	0.0	0.0	0.0
3	NONE (w/o PVC)	416	22.9	10.8	9.7	25.0	4.7	11.9	2.6	9.8	0.0
4	MgO-ZnO	439	9.3	10.3	9.6	34.3	12.0	8.8	1.3	6.5	4.6
5	MgO-ZnO	400	7.2	5.5	5.1	17.2	46.1	6.7	1.5	8.1	0.0
6	ZnO-TiO ₂	414	5.4	5.9	5.5	17.6	35.2	7.8	0.0	6.7	0.0
7	ZnO-TiO ₂	410	5.7	4.9	5.0	20.5	53.3	6.3	2.0	0.0	0.0
8	TiO ₂ -SiO ₂	410	8.3	4.6	4.6	16.5	52.8	5.0	0.7	7.6	0.0
9	ZnO-Al ₂ O ₃	400	4.5	4.6	4.2	12.4	56.2	7.6	2.1	5.0	0.0
10	MgZrO ₄	438	8.7	8.2	7.9	37.4	13.5	9.0	0.1	9.5	4.8
11	MgTiO ₃	400	6.1	3.9	3.6	13.5	57.9	6.4	0.7	5.8	0.0
12	Fe ₂ O ₃	410	7.2	14.2	14.2	19.7	36.7	5.1	0.8	0.7	0.0
13	CuO	400	8.5	7.0	6.3	41.5	28.6	6.3	1.0	0.9	0.0
14	Montmorillonite K 10	400	3.0	3.8	3.6	4.9	82.0	2.7	0.0	0.0	0.0
15	ASR Char	400	2.8	1.5	1.2	2.5	90.4	1.6	0.0	0.0	0.0

TABLE 4. GC ANALYSIS OF THE SECOND AND THIRD GAS SAMPLES, AT 500 °C AND 650 °C, RESPECTIVELY. STATISTICAL DISTRIBUTION OF PRODUCTS FROM RUNS 1 - 15

GASES	SECOND SAMPLE		THIRD SAMPLE	
	MEAN (%)	STANDARD DEVIATION	MEAN (%)	STANDARD DEVIATION
Methane	14.3	1.39	41.5	2.08
Ethylene	9.7	2.15	11.9	1.05
Ethane	13.6	0.71	13.25	1.43
Propylene	32.5	2.16	19.25	1.87
Methyl Chloride	2.33		0.52	
Butene	12.6	1.55	8.59	0.88
Butadiene	0.21		2.27	
Unknown 1	4.32		0.5	
Unknown 2	8.95	2.02	0.35	



REACTION	ACTIVATION ENERGY (cal/mole)	PRE-EXPONENTIAL (1/min)
1	3000	0.13
2	3000	0.10
3	5500	0.14
4	14000	0.004
5	7000	0.08
6	5000	10.0

X-RAY CHARACTERIZATION OF TIRE DERIVED PARTICLES RESULTING FROM DIFFERENT SOLVENTS

Ricky C. Cummings, Charles B. Smithhart,* Jeff Quin, and David L. Wertz
Department of Chemistry & Biochemistry
and
Center for Coal Product Research
University of Southern Mississippi
Hattiesburg, MS 39406-5043 USA

Key Phrases: Tire derived particle, x-ray spectroscopy, inorganics

INTRODUCTION

Currently, 200 million scrap tires are being annually stockpiled, landfilled, or illegally dumped, with ca. 50 million scrap tires being recycled in a variety of ways. The current disposal methods are causing numerous short-term environmental problems. Whole tires occupy large amounts of space and may "float" or rise to the top of landfills, causing puncturing of the landfill cover. In an attempt to prevent floating, many landfills require that the scrap tires be shredded, a process which is energy intensive and wasteful. Scrap tire stock piles produce large health risks by providing a place for rodents and mosquitos to breed -- aiding in the spread of diseases.¹ Large stockpile fires have also broken out in major cities in Florida, Texas, Virginia, and Washington. These fires are long lasting and produce unwanted smoke into the environment.² For many reasons, the recycling of scrap tires is desirable.

Current attempts to upgrade the hydrocarbons in the scrap tires to produce oils and carbon materials have met with limited success.³

Scrap tires represent a "renewable" source for feedstock for chemicals and for energy, containing $3 \cdot 10^5$ BTU's per tire and high abundances of carbon and hydrogen.

Scrap tires also contain several inorganics which are impregnated into the rubbery portion and iron (with a brass surface) from their steel belts. These inorganics are likely to hinder the recycling of the rubbery portion of the tires.⁴ Their removal is necessary because when combusted in a conventional boiler, the inorganic will cause air pollution and/or boiler scale build up as well as interfering with various catalytic processes.

Removal of the inorganics is the subject of this research.

EXPERIMENTAL

Whole tires were cut into 1 inch by 1 inch squares. These tire chunks were then treated with different liquids (n-methyl pyrrolidinone, nitric acid, 50% hydrogen peroxide, and sulfuric acid) by placing the tire chunks in the liquids and stirring at ambient conditions. A tire derived particle (TDP) was then recovered by filtration. After drying, the particles were placed in plastic cups, covered with a thin mylar film, and placed in the sample chamber of our x-ray spectrometer for analysis.

Our x-ray protocol involved collecting intensity at increments of $\Delta 2\theta = 0.025^\circ$ over the range from $2\theta = 10.00^\circ$ to $2\theta = 110.00^\circ$ using a sample spinner.

X-ray fluorescence spectroscopy (XRF) has been an established research tool for at least seventy-five years in the area of elemental analysis.⁵ Wavelength dispersive XRF has been used in this project to monitor the removal of the inorganic species noted above by the several processes we have developed. For each WDXRF spectrum, the choice of the monochromator used to disperse the secondary X rays emitted by the analyte element(s) in the sample and the detector used to measure the secondary X rays are important. For the

WDXRF spectra reported herein, a graphite crystal monochromator ($d = 3.38 \text{ \AA}$) was used to disperse the secondary X rays emitted by the various analytes in the samples. Both a gas proportional counter (gpc) and a scintillation counter (sc) were used to detect and collect the secondary X rays. The former has a high efficiency for collecting "softer" X rays ($\lambda > 1.25 \text{ \AA}$), while the latter has a high efficiency for collecting hard X rays ($\lambda < 1.25 \text{ \AA}$).

Wavelength dispersive x-ray fluorescence spectroscopy was used to measure the abundances of the inorganic species in the tire before processing and to analyze the removal efficiency of the different liquids for these inorganics.

RESULTS AND DISCUSSION

The resulting TDP's had surface areas in 0.1-2.0 mm^2 range.

ANALYSIS OF THE TIRE CHUNKS. The wavelength dispersive XRF spectrum (using Cr radiation and the gas proportional counter) of an untreated tire chunk is shown in Figure 1. The spectrum contains peaks due to zinc ($\lambda K_{\alpha} = 1.436 \text{ \AA}$), calcium ($\lambda K_{\alpha} = 3.359 \text{ \AA}$), and sulfur ($\lambda K_{\alpha} = 5.373 \text{ \AA}$). The chromium peak ($\lambda = 2.290 \text{ \AA}$) in the WDXRF spectrum is due to the use of chromium as the exciting radiation (tube) for the experiments. Chromium produces "soft" X rays which do not penetrate deeply into the rubbery portion of the scrap tire. Consequently, the x-ray peak due to iron ($\lambda K_{\alpha} = 1.937 \text{ \AA}$) is barely discernible in the spectrum.

Shown in Figure 2 is the WDXRF spectrum of the same tire chunk using a scintillation counter rather than a gas proportional counter for x-ray detection and a molybdenum ($\lambda K_{\alpha} = 0.711 \text{ \AA}$) radiation source. A small peak due to bromine ($\lambda K_{\alpha} = 1.041 \text{ \AA}$) is clearly discernible, along with the Mo peak. There is, of course, no chromium peak in this spectrum.

When the steel belts were removed from the rubbery section of the tire, ground to a powder, and then submitted to our XRF analysis, the peaks due to iron, copper and zinc are clearly discernible.

TREATMENT WITH THE PROCESS LIQUIDS. The four liquids had different effects on the tire chunks. The n-methyl pyrrolidinone is absorbed into the tire chunk, causing the rubbery portion of the tire to swell. NMP cleaves the adhesion between the rubbery portion of the tire and the steel belts, while the tire chunk becomes very brittle and easily grindable. It proved difficult to recover the NMP from the tire chunks.

Concentrated nitric acid degrades the tire chunk into particles and dissolves the steel belts. The WDXRF spectrum of the resulting TDP is shown in Figure 3. Comparison of the WDXRF spectra of the untreated tire to that of the TDP indicates that the zinc, calcium, and sulfur abundances have been drastically reduced in the TDP by the nitric acid treatment at ambient conditions. Lengthening the time of treatment results in complete removal of the unwanted inorganics.

Figure 4 shows the WDXRF spectrum of the residue produced by evaporating the nitric acid filtrate to dryness. The characteristic peaks due to the metal species are provided in this spectrum, verifying the absence of the unwanted inorganics in the TDP. The large iron peak is due to the fact that the nitric acid dissolves the steel belts.

Comparison of the intensities of the zinc peaks in Figures 1, 3, and 4 indicates that the mass balance for zinc in these three samples is not well established and/or that the enhancement/absorption effects for the Zn peaks cannot be ignored in these samples.

Treatment with 50% hydrogen peroxide at ambient conditions does not degrade the tire chunks nearly as rapidly as does the nitric acid treatment. This treatment also extracts the inorganics, which are subsequently found in the residue evaporated from the filtrate. This method also attacks the steel belts, as evidenced by the large iron peaks in the WDXRF of the residue from the evaporate.

Concentrated sulfuric acid degrades the tire chunks almost as well as the nitric acid at ambient conditions but does not dissolve the steel belts. The steel belts may then be removed easily (and essentially in tact) from the rubbery portion of the tire and collected on the stir bar. Comparison of the WDXRF intensities indicates that the sulfuric acid did not remove the zinc, calcium, or sulfur at ambient conditions.

A summary of current results is presented in Table I. Additional results will be discussed.

CONCLUSIONS

Tires chunks may be treated at ambient conditions with different liquids, producing different effects. The unwanted inorganics can be extracted from the tire chunks, leaving a TDP with a high carbon and hydrogen content and a greatly reduced surface area. Wavelength dispersive x-ray fluorescence spectroscopy may be used to monitor the reduction in abundances of each of the unwanted inorganics. Altering the conditions of the WDXRF experiment provides different information about the distribution of inorganics in the tire chunk and the TDP's.

REFERENCES

1. U.S. Environmental Protection Agency. **Scrap Tire Handbook: Effective Management Alternatives to Scrap Tire Disposal in Illinois, Indiana, Michigan, Minnesota, Ohio, and Wisconsin.** 1994.
 2. Transportation Research. **Uses of Recycled Rubber Tires in Highways.** 1994.
 3. Liu, Z., Zondlo, J.W., and Dadyburjor, D.B., **Energy and Fuels**, 1994 (8) 607.
 4. Sopek, D.J. and Justice, A.L. in "Clean Energy from Waste & Coal", M.R. Khan, Am. Chem. Soc., 1991.
 5. Jenkins, R., "X-Ray Spectrometry", John Wiley & Sons, NY, 1988.
 6. Rousseau, R. M., "A Practical XRF Calibration Procedure", 43rd Annual Denver X-Ray Conference, Steamboat Springs, CO. 1994.
- DOE-EPSCoR Graduate Fellow.

TABLE I. EFFECTS OF LIQUIDS OF SCRAP TIRE PARAMETERS.

LIQUID USED	INORGANIC REMOVAL			FATE OF STEEL BELT ADHESIONS	CONDITION OF LIQUID
	Zn	Ca	S		
NMP	no effect			cleaved	absorbed into rubber
nitric acid	E	E	E	dissolved	recyclable
sulfuric acid	no effect			cleaved	recyclable
hydrogen peroxide	E	E	E	dissolved	recyclable

E Extracted by the liquid.

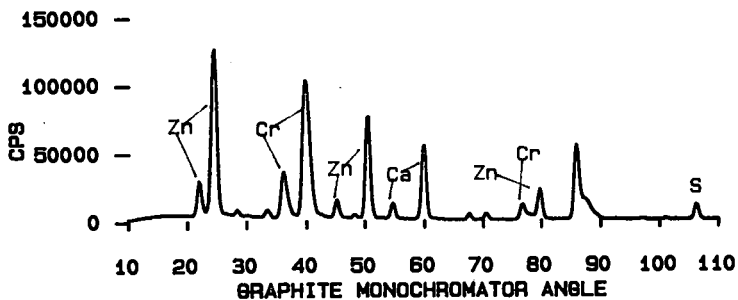


FIGURE 1. WDXRF SPECTRUM OF UNTREATED TIRE CHUNKS; Cr/GPC.

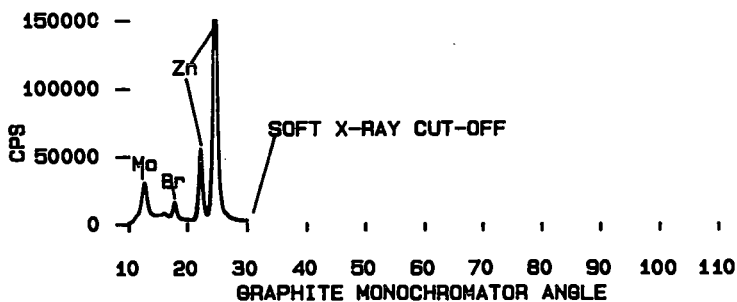


FIGURE 2. WDXRF SPECTRUM OF UNTREATED TIRE CHUNK; Mo/SC.

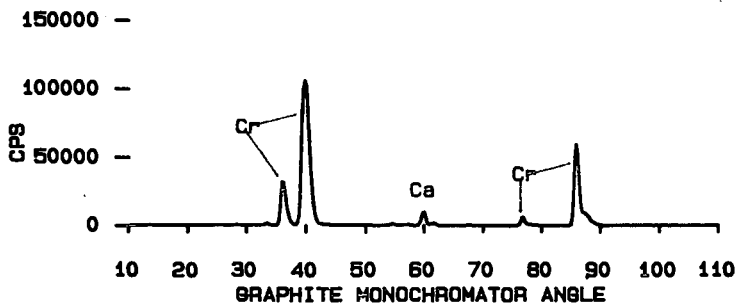


FIGURE 3. WDXRF SPECTRUM OF TDP FROM THE NITRIC ACID TREATMENT; Cr/GPC.

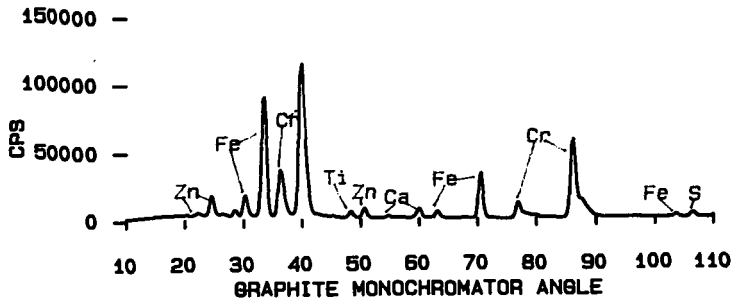


FIGURE 4. WDXRF SPECTRUM OF RESIDUE FROM NITRIC ACID TREATMENT; Cr/GPC.

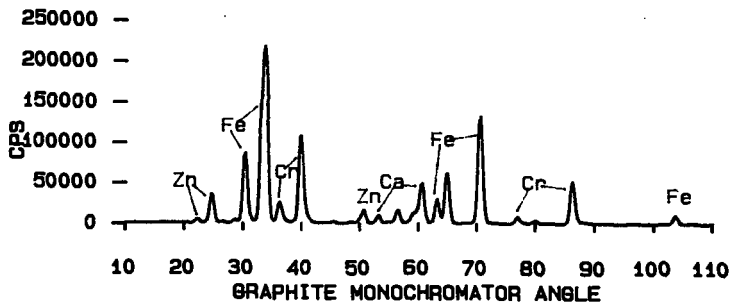


FIGURE 5. WDXRF SPECTRUM OF THE FILTRATE RESIDUE FROM THE 50% HYDROGEN PEROXIDE TREATMENT; Cr/GPC.

THE GROWING NEED FOR RISK ANALYSIS

C.C. Lee and G.L. Huffman
Risk Reduction Engineering Laboratory
U.S. Environmental Protection Agency
Cincinnati, OH 45268

Keywords: Risk analysis, Risk assessment, Risk management

ABSTRACT

Risk analysis has been increasingly receiving attention in making environmental decisions. For example, in its May 18, 1993 Combustion Strategy announcement, EPA required that any issuance of a new hazardous waste combustion permit be preceded by the performance of a complete (direct and indirect) risk assessment. This new requirement is a major challenge to many engineers who are involved in waste incineration activities. This Paper presents the highlights of what is required for a risk analysis from a practical engineering point of view. It provides the regulatory basis for it to provide the rationale as to why risk analysis is needed.

INTRODUCTION

"Nothing would be done at all if a man waited till he could do it so well that no one could find fault with it"--Cardinal Newman. Cardinal Newman's statement is very pertinent to the subject of "Risk Analysis." The assessment of environmental risks posed to human health is an incredibly complex undertaking. Because of this complexity, it is very difficult to do much more than identify sources and effects of potential concern and, in a rough manner, to quantify transport along major pathways (Martin-86). In addition, risk analysis has been basically developed by scientists. This makes it more difficult for engineers to apply the risk models developed by these scientists to their "real-world" waste treatment problems, because of the different disciplines and terminologies involved.

Basically, the authors used the documents contained in the "References Section" to derive the information for this Paper. The objective of this Paper is to summarize the highlights of what is required for a risk analysis from a practical engineering point of view. It emphasizes the documentation of risk analysis requirements from various environmental statutes. The purpose is to establish the regulatory basis relative to why risk analysis is needed, and how risk analysis should be conducted. It is believed that the understanding of the statutory provisions is important and that the only way to formulate the proper risk analysis approach is to comply with the regulatory requirements under the specific environmental laws that apply. For example, in the past, risk assessments were not required for obtaining a hazardous waste incineration permit. However, in its May 18, 1993 Combustion Strategy announcement, EPA required that any issuance of a new hazardous waste combustion permit be preceded by a complete direct and indirect risk assessment (EPA-93/5). This new requirement is a major challenge to many engineers who are involved in waste incineration activities.

REGULATORY BASIS FOR RISK ASSESSMENT

Risk is the probability of injury, disease, or death under specific circumstances (Lee-92/6). Risk assessment is a cornerstone of environmental decision-making. EPA defines risk assessment as: (1) the determination of the kind and degree of hazard posed by an agent (such as a harmful substance); (2) the extent to which a particular group of people has been or may be exposed to the agent; and (3) the present or potential health risk that exists due to the agent (Lee-92/6). Risk assessment is a complex process by which scientists determine the harm that an individual substance can inflict on human health or the environment. For human health risk assessment, the process takes place in a series of four major steps as follows (EPA-90/6; NAC-83):

- (1) Hazard identification: In identifying hazards, two kinds of data are gathered and evaluated: (A) data on the types of health injury or disease that may be produced by a chemical; and (B) data on the conditions of exposure under which injury or disease is produced. The behavior of a chemical within the body and the interactions it undergoes with organs, cells, or even parts of cells may also be characterized. Such data may be of value in answering the ultimate question of whether the forms of toxicity known to be produced by a substance in one population group or in experimental settings are also likely to be produced in humans.
- (2) Dose-response assessment: The next step in risk assessment describes the relationship between the amount of exposure to a substance and the extent of toxic injury or disease. Even where good epidemiological studies have been conducted, reliable quantitative data on exposure in humans are rarely available. Thus, in most cases, dose-response relationships must

be estimated from studies in animals, which immediately raises three serious problems: (A) animals are usually exposed at high doses, and effects at low doses must be predicted by using theories about the form of the dose-response relationship; (B) animals and humans often differ in susceptibility (if only because of differences in size and metabolism); and (C) the human population is heterogeneous, so some individuals are likely to be more susceptible than the average.

- (3) **Human exposure assessment:** Assessment of human exposure requires estimation of the number of people exposed and the magnitude, duration, and timing of their exposure. The assessment could include past exposures, current exposures, or exposures anticipated in the future. In some cases, measuring human exposure directly, either by measuring levels of the hazardous agents in the ambient environment or by using personal monitors, is fairly straightforward. In most cases, however, detailed knowledge is required of the factors that control human exposure, including those factors that determine the behavior of the agent after its release into the environment.
- (4) **Risk characterization:** The final step in risk assessment combines the information gained and analysis performed during the first three steps to determine the likelihood that humans will experience any of the various forms of toxicity associated with a substance. The risk characterization then becomes one of the factors considered in deciding whether and how the substance will be regulated.

In the 1980s, as health risk assessment became more widely used across U.S. EPA programs, the need for consensus and consistency in the areas of hazard identification and dose-response assessment became clear. In 1986, EPA work groups were convened to establish consensus positions on a chemical-by-chemical basis for those substances of common interest and to develop a system for communicating the positions to EPA risk assessors and risk managers. This effort resulted in the creation of EPA's Integrated Risk Information System (IRIS) in 1986. In 1988, the IRIS was made available to the public.

IRIS currently contains summaries of EPA human health hazard information that support two of the four steps--hazard identification and dose-response evaluation--of the risk assessment process. It currently contains information on approximately 500 specific substances. Questions such as "what is the potential human health hazard of exposure to benzene?" and "what are the possible cancer and/or non-cancer effects?" can find answers from IRIS (EPA-93/1).

A key factor affecting the regulatory coverage of a statute is the definition of the substances subject to regulation. The statutes use several descriptive terms, not necessarily having the same meaning, to identify "harmful substances." These include pollutant, toxic pollutant, hazardous substance, contaminant, hazardous material, and hazardous waste. The Toxic Substances Control Act (TSCA), for example, defines "chemical substances" and "mixtures" subject to regulation if certain criteria are met; the Federal Insecticide, Fungicide, and Rodenticide Act (FIFRA) and the Marine Protection, Research, and Sanctuaries Act (MPRSA) specify categories of substances [FIFRA defining "pesticides," and MPRSA "materials"].

In general, three aspects of risk are addressed in each statute. They are: type of harm, type of risk, and required considerations between the chemical and the harm that may result (Martin-86).

Type of Harm: The type of harm is usually explicitly described by terms that define the chemicals or the substances to be addressed (e.g., a hazardous substance that may cause injury to health or the environment). The harm components of a statute's risk definition generally consist of a description of an undesired outcome (death, injury) and/or a description of the population (public, wildlife) at risk or the objective of the regulation, such as protection of the environment.

Type of Risk: Considering risk when developing federal regulations encompasses the probability of harm occurring. The probability of harm presented by a chemical may be considered zero, insignificant, or significant. A term such as "significant risk" will then be addressed by the rule-making process.

Required Considerations: The statutory language may guide the designation and setting of technical or control standards for explicitly specifying a basis for making regulatory decisions and also for indicating what factors must be, may be, or may not be considered when developing regulations. The statutes discuss the amount of protection or risk reductions to be addressed through the issuance of standards "necessary,"

"adequate," or "sufficient" to protect health or the environment by providing detailed guidance (e.g., ample margin of safety) and/or by prescribing partial factors (e.g., risk and cost) that must be considered.

REGULATORY BASIS FOR RISK MANAGEMENT

EPA is responsible for implementing environmental statutes. Although, the statutes generally do not prescribe risk assessment methodologies, many environmental laws do provide very specific risk management directives, and these directives vary from statute to statute. EPA defines risk management as the process of evaluating alternative regulatory and non-regulatory responses to risk and selecting among them. The selection process necessarily requires the consideration of legal, economic and social factors (Lee-92/6).

Statutory risk management mandates can be roughly classified into three categories: (1) pure risk; (2) technology-based standards; and (3) reasonableness of risk balanced with benefits (EPA-93/1).

(1) Pure-Risk Standards

Pure-risk standards are, sometimes, termed zero-risk standards. This category allows an adequate margin of safety, however, requires the protection of public health without regard to technology or cost factors. For example, the National Ambient Air Quality Standards (NAAQS) of the Clean Air Act belong to this category.

(2) Technology-Based Standards

Technology-based environmental standards focus on the effectiveness and costs of alternative control technologies rather than on how control actions could affect risks. For example, industrial water pollution standards, where the installation of a single control system can reduce risks from a variety of different pollutants, belong to this category.

Consider the several technology-based standards in the Clean Water Act. The Act requires industries to install several levels of technology-based controls for reducing water pollution. These include best practicable control technology, best conventional technology, and best available technology economically achievable for existing sources. New sources are subject to the best demonstrated control technology. Total costs, age of equipment and facilities, processes involved, engineering aspects, environmental factors other than water quality, and energy requirements are to be taken into account in assessing technology-based controls.

(3) No Unreasonable Risk

This category calls for the balancing of risks against benefits in making risk management decisions. The following are two examples in this category:

- The Federal Insecticide, Fungicide, and Rodenticide Act requires EPA to register (license) pesticides which, in addition to other requirements, it finds will not cause unreasonable adverse effects on the environment. The phrase refers to any unreasonable risks to man or the environment taking into account the economic, social, and environmental costs and benefits of the use of any pesticide.
- Under the Toxic Substances Control Act, EPA is mandated to take action if it finds that a chemical substance presents or will present an unreasonable risk of injury to health or the environment. This includes considering the effects of such a substance on health and the environment and the magnitude of the exposure of human beings and the environment to such a substance; the benefits of such a substance for its various uses and the availability of substitutes for such uses; and the reasonably ascertainable economic consequences of the rule, after consideration of the effect on the national economy, small businesses, technological innovation, the environment, and public health.

THE ROLE OF COMPARATIVE RISK ANALYSIS

EPA's support for using comparative risk analysis to help set its regulatory priorities has been no secret. Unlike risk assessment, which for years has provided regulators the basis for deciding whether or not an individual substance needs to be controlled, comparative risk analysis and its derivative, relative risk, have arrived on the scene only recently. Very simply described, comparative risk analysis is a procedure for ranking environmental problems by their seriousness (relative risk) for the purpose of assigning them program priorities. Typically, teams of experts put together a list of problems; then,

they sort the problems by types of risk--cancer, non-cancer health, materials damage, ecological effects, and so on. The experts rank the problems within each type by measuring them against such standards as the severity of effects, the likelihood of the problem occurring among those exposed, the number of people exposed, and the like. The relative risk of a problem is then used as a factor in determining what priority the problem should receive. Other factors include statutory mandates, public concern over the problem, and the economic and technological feasibility of controlling it.

EPA's Science Advisory Board urged the Agency to order its priorities on the basis of reducing the most serious risks. The Board argued, in part ... There are heavy costs involved if society fails to set environmental priorities based on risk. If finite resources are expended on lower priority problems at the expense of higher priority risks, then society will face needlessly high risks. If priorities are established based on the greatest opportunities to reduce risk, total risk will be reduced in a more efficient way, lessening threats to both public health and local and global ecosystems....(EPA-93/1).

THE ROLE OF RISK COMMUNICATION

Basically, risk communication deals with the approaches to communicate with the public on various environmental issues. Some recommended communication checklist items are provided as follows (EPA-90/6): (1) Be prepared; (2) Review the facts; (3) Anticipate likely questions; and (4) Consider what the audience wants to know.

THE ROLE OF RISK UNCERTAINTY

Uncertainty means the quality or state of having possible variations. In risk analysis, uncertainty factors include: (1) the variation in sensitivity among the members of the human population; (2) the uncertainty in extrapolating animal data to the case of humans; (3) the uncertainty in extrapolating from data obtained in a study that is of less-than-lifetime exposure; (4) the inability of any single study to adequately address all possible adverse outcomes in humans.

SUMMARY

By way of summarizing, the following key questions concerning the above-described "risk" terms might be asked:

- (1) Risk assessment: What do we know about risk? or how risky is this situation?
- (2) Risk management: What do we wish to do about risk? or what shall we do about it?
- (3) Comparative risk: What is the ranking (priority) of the various risks?
- (4) Risk communication: What and how should a risk assessor communicate with the public on risk analysis?
- (5) Risk uncertainty: What is the quality or state of having possible variations in conducting risk analysis?

REFERENCES

(EPA-89/3), "Risk Assessment Guidance for Superfund: Volume II - Environmental Evaluation Manual," EPA540-1-89-001, March 1989.

(EPA-90/1), "Methodology for Assessing Health Risks Associated with Indirect Exposure to Combustor Emissions, Interim Final," EPA600-6-90-003, January 1990.

(EPA-90/6), "Risk Assessment, Management and Communication of Drinking Water Contamination," EPA625-4-89-024, June 1990.

(EPA-91/12), "Risk Assessment Guidance for Superfund: Volume I - Human Health Evaluation Manual (Part B, Development of Risk-based Preliminary Remediation Goals), EPA540-R-92-003, Publication 9285.7-01B, December 1991.

(EPA-93/1), "The ABCs of Risk Assessment," EPA Journal, EPA175-N-93-0014, Volume 19, Number 1, January/February/March 1993.

(EPA-93/5), "Environmental News: EPA Administrator Browner Announces New Hazardous Waste Reduction and Combustion Strategy," May 18, 1993.

(EPA-94/4), "Exposure Assessment Guidance for RCRA Hazardous Waste Combustion Facilities," EPA530-R-94-021, April 1994.

(Lee-92/6), "Environmental Engineering Dictionary," C.C. Lee, June 1992.

(Martin-86), "Hazardous Waste Management Engineering," Edward J. Martin and James H. Johnson, Jr.), Van Nostrand Reinhold Company, New York, 1986.

(Martin-86/2), "Incinerator Risk Analysis Presentation to: Incinerator Permit Writer's Workshop," Edward J. Martin, Peer Consultants, Inc., February 4, 5, and 6, 1986.

(NAC-83), "Risk Assessment in the Federal Government: Managing the Process," Committee on the Institutional Means for Assessment of Risks to Public Health, Commission on Life Sciences, National Research Council, Established by National Academy Council (NAC), National Academy Press, 1983.

(NIOSH-84/10), "Personal Protective Equipment for Hazardous Materials Incidents: A Selection Guide," U.S. Department of Health and Human Services, Public Health Service, Centers for Disease Control, National Institute for Occupational Safety and Health (NIOSH), Division of Safety Research, Morgantown, West Virginia 26505, October 1984.

(NRT-87/3), "Hazardous Materials Emergency: Planning Guide," National Release Team (NRT), NRT-1, March 1987.

EVALUATION OF A BIOMASS DERIVED OIL FOR USE AS ADDITIVE IN PAVING ASPHALT

J. Houde Jr., I. Clelland, H. Sawatzky, Energy Research Laboratories, CANMET, Natural Resources Canada, 555 Booth St., Ottawa, Ont., Canada, K1A 0G1. E-mail: jean.houde@x400.emr.ca

Keywords: paving asphalt, additive, antistripping

INTRODUCTION

Treatment and disposal costs of sewage sludge can represent up to 50% of a municipality's annual wastewater treatment budget. Sewage sludge (30% solids) accounts 5% of Canadian landfill by weight, and the ever increasing volume of sludge coupled with the decreasing options available for disposal creates a growing problem for major municipalities. Current disposal options are agricultural application, incineration and landfill. Concern about heavy metal migration and public pressure to find a local solution has severely curtailed the spreading of sludge on agricultural land. Incineration is the major option for larger centres but the relatively high cost for incineration, ranging from \$350 to \$1000/t dry sludge, has caused a great deal of interest in methods of improving the cost effectiveness of incineration or in new equivalent technologies. The high cost and more stringent environmental regulations for incinerating municipal sludges have led to developing more efficient sludge management technologies that are not agricultural based.

The Wastewater Technology Centre of Environment Canada has been developing one such technology since 1982. The thermoconversion process shown in Fig. 1 involves low temperature treatment of sludge to liquid and solid fuel products (1). A key technical feature of the sludge conversion is the formation of a byproduct oil (2) referred to as sludge derived oil (SDO). In 1989, Enersludge Inc., Wastewater Technology Centre and CANMET's Energy Research Laboratories (ERL) of Natural Resources Canada undertook a joint R&D program to be conducted at ERL to investigate promising utilization options for the SDO. SDO is a black, viscous high-boiling (>150°C) organic liquid with a characteristic odour. Initial characterization tests led to investigating the use of SDO as a feedstock material for introduction into a refinery stream. Its average chemical structure is that of a large complex molecule, with a hydrocarbon skeleton and functional groups containing nitrogen (pyrroles, amides) and oxygen (esters). Such structures, which indicate protein origins, tend to be very polar. The relatively high concentration of polar groups in SDO, especially the abundance of nitrogenous groups, and its incompatibility with most distillate hydrocarbons except heavy aromatic gas oils, as discovered in more extensive characterization testing, indicated a more appropriate role as an asphalt additive. This paper describes the work done at ERL to develop SDO for antistripping applications.

COMPATIBILITY

The affinity of SDO for heavy petroleum derived materials was initially investigated by blending equal amounts of SDO in each of ROSE[®] (residual oil supercritical extraction) residue (3) and CANMET hydrocracking pitch (4). Both were observed to be completely miscible and formed stable viscous blends. The same was then observed with SDO and pentane-precipitated Athabasca bitumen asphaltenes.

Asphalt cement (A/C), a petroleum product made from the fraction that has a boiling point greater than approximately 350°C, contains many polar components including sulphur and nitrogen containing compounds. SDO was found to be compatible with A/C as indicated by the high ductility of SDO and commercial asphalt blends. Incompatibility in an asphalt blend causes a drastic decrease in ductility that is easily detected in comparison to commercial A/C. Ductility is determined by measuring the distance a fixed shape of A/C will stretch at a fixed temperature and rate of elongation until it breaks.

The results of this preliminary investigation as well as the characterization indicated SDO was compatible with A/C. Further, the SDO showed evidence of strong affinity for asphaltenes in asphalt. The high nitrogen content of SDO is desirable for improving of adhesion to aggregate.

ROAD ASPHALTS

Asphaltic concrete road pavement is made from a mix of aggregate (sand, gravel and crushed stone) held together by 5% to 10% on a weight basis of A/C. Government transportation agencies have developed road pavement specifications and are also the largest buyers of road pavement. Their specifications include the hardness of the A/C, its ductility, viscosity, flash point, resistance to stripping and performance after simulated road paving and handling evaluations. Table 1 lists the American Society for Testing and Materials (ASTM) test methods typically used to assess commercial A/C's.

Currently in Canada, A/C is primarily graded on its hardness as measured by penetration, reported as the measured penetration by a needle into a sample of A/C of specified temperature

for controlled time and force (weight) on the needle. Asphalt of 85 dmm (tenths of millimetres) to 100 dmm, i.e., 85/100 penetration, is considered hard, whereas 150/200 penetration is soft.

ANTISTRIPPING ADDITIVE

The resistance to stripping of the A/C from the surface of the aggregate is an important specification for the performance of asphalt pavement and is monitored by the buyers of asphalt pavement. Since A/C does not adhere well to certain aggregates, transportation agencies specify the use of antistripping agents when using these particular aggregates. Stripping involves complex processes which are still not fully understood. Several factors influence the sensitivity of asphalt concrete mix to stripping [5]. For this phenomenon to occur, free water must be present.

Jamieson aggregate (Ontario, Canada) which is prone to stripping and listed by the Ministry of Transport of Ontario (MTO) as requiring at least 1% antistripping agent in the A/C, was chosen to evaluate the antistripping performance of SDO in A/C blends. ASTM test method D-1664¹, the test method for evaluating coating and stripping of bitumen-aggregate mixtures, requires a 95% coverage in static immersion tests to meet specifications.

To demonstrate the stripping resistance of SDO in A/C blends, three commercial A/Cs and various concentrations of SDO were used with Jamieson aggregate as shown in Fig. 2. The results are an average from the visual stripping evaluations of a panel of five evaluators. The coverage of the aggregate by the A/C increased from about 60% (for the first two A/Cs) to above 90% as SDO was added. The retained coverage of the third A/C, with no SDO, increased from about 40% to above 90% as in the above case. Further, the performance of an A/C with one of the commercial antistripping agents, Alkazine-O, recommended by the MTO is shown for comparison (80% retained coating at the 1 wt % level). Under these conditions, SDO has antistripping performance equal to or in excess of that given by at least one commercial agent, and can be used to have coverage in excess of MTO specifications.

Sources of SDO other than the Atlanta SDO (undigested sewage sludge derived oil) were also evaluated for performance as antistripping agents. These samples were also obtained from bench-scale experiments using Highland Creek (Toronto, Canada) sewage sludge, an undigested sludge, and Hamilton sewage sludge, a digested sludge, supplied by the Wastewater Technology Centre. A digested sludge is one that has been subjected to anaerobic bacterial digestion. An SDO from digested sludge has a reduced nitrogen content. In Fig. 3, several concentrations of these two SDOs are compared with commercial antistripping agents: Alkazine-O, Redicote AP and Redicote 82S. Some of these commercial agents are as effective as the SDO at approximately half the concentration. Comparison of Highland Creek SDO and Hamilton SDO (undigested versus digested sludges) as antistripping agents shows a parallel, but slightly less effective performance curve for the digested SDO, indicating the significance of the nitrogen content of SDO as a factor in adhesion to aggregate.

The use of antistripping additive may cause significant modifications to other performance properties of asphalt cement. The other properties of asphalt cement susceptible to modifications were also assessed. Candidate blends of asphalt cement with SDO and commercial antistripping agents were evaluated for asphalt cement performance specifications in Table 2. Blends of 2% Redicote 82S were compared with SDO blends as well as several other commercial antistripping agents. These results indicated the performance of SDO at 5% does modify the asphalt cement test results, in particular the loss of volatiles in the thin film oven test and the penetration. The changes to the penetration of the asphalt cement can be modified by a change in the distillation temperature of the SDO fraction or a change in the consistency of the A/C. However, there may be a limit to the acceptability of a change in penetration caused by an additive unless the A/C is very hard. It should be noted that the use of only 2% SDO with the A/C3 in Fig. 2, was successful for all specifications monitored. Further, the viscosity of the SDO containing asphalt cement easily met the MTO criteria.

In an effort to further define the antistripping performance curve, SDO was again tested by the stripping immersion method including the 3 wt % additive level. The results in Fig. 4 show that the 3 wt % additive level was as effective as the 5 wt % additive level in both 85/100 and 150/200 penetration A/C4. The 3 wt % additive level resulted in less change of the A/C's consistency, as shown in Table 3. In another phase of testing, a one year old SDO sample was compared to a freshly obtained sample. There was no significant difference in effectiveness as an antistripping agent between the SDO samples, indicating the stability of the product.

¹ Summary of ASTM D-1664 : The selected and prepared aggregate is coated with the bitumen at a specified temperature appropriate to the grade of bitumen used. The coated aggregate is immersed in distilled water for 16 to 18 h. At the end of the soaking period, and with the bitumen-aggregate mixture under water, the total area of the aggregate on which the bituminous film is retained is estimated visually as $\geq 95\%$.

MARSHALL TEST

The next logical step was to test how SDO as an A/C additive compared to a commercial additive in the asphalt concrete. One of the standard testing methods commonly used is known as the Marshall test. The A/C and selected aggregate are mixed hot to produce an asphalt concrete which is compacted by a laboratory compactor, simulating the roller compaction the concrete would receive in the field. The cooled asphalt concrete sample is tested for strength and resistance to plastic flow with an applied lateral force.

A standard HL-3 mix design was used for manufacturing all specimens to be evaluated. The ratio of coarse to fine aggregate was 40/60. Each specimen contained 5% A/C. Specimens were manufactured according to MTO LS-261 and tested according to MTO LS-263 and LS-264 procedures for resistance to plastic flow using Marshall apparatus and theoretical maximum relative density, respectively. Table 4 gives the results for the Marshall stability of 5% SDO and 2% Redicote 82S blended in 85/100 penetration A/C. Three duplicate determinations were done on each sample. The results show that the SDO blend performed as well as the commercial antistripping agent, Redicote 82S. The SDO addition did not lower the Marshall stability of the samples studied.

RECYCLED ASPHALT

When asphalt pavement is exposed to atmospheric conditions for several years, it degrades by becoming harder and more brittle. For this reason, asphalt pavement must be replaced or drastically repaired at the end of its typical age of 12 years. One notable effect of aging on asphalt cement is the increase in the asphaltene content. Attempts at softening aged asphalt cement by adding low viscosity high-boiling petroleum oils were unsuccessful because these oils do not accommodate the increase in asphaltene content. A successful agent for softening or rejuvenating aged asphalt cement must be able to disperse or peptize the asphaltenes. In general, very soft asphalts, referred to as fluxes, are used to rejuvenate aged asphalts because they can absorb the effect of the increased asphaltenes. Given the excellent ability of SDO to dissolve the CANMET residue, the ROSE[®] residue, and the Athabasca asphaltenes, it was expected that SDO would rejuvenate aged asphalt. Further, the softening and reduction in penetration observed in blends of SDO and virgin asphalt cement are also desirable.

A sample of aged asphalt cement was obtained from a local asphalt pavement replacement operation. Milled asphalt pavement was extracted with toluene and the aged asphalt cement was recovered by evaporation. The aged asphalt cement was blended with SDO. The penetrations and kinematic viscosities are shown in Table 5.

Further, Bow River crude asphalt of 454°C was blended with the aged asphalt. Bow River asphalt is very soft and is considered to be a high quality flux, which is ideal for rejuvenating asphalt. The results indicate that hard, aged asphalt cement of 30 dmm penetration can be softened to make the equivalent of 85/100 penetration grade asphalt cement. Only 12% SDO was required to make this penetration whereas more than 22% Bow River flux is required. However, the viscosity of 22% Bow River flux in asphalt cement is just above the MTO kinematic viscosity minimum of 280 cSt. If more Bow River were added to make the 85/100 penetration grade of asphalt cement, it would probably just fail the viscosity specification.

SDO performance in hot mixed recycling was investigated using the thin film oven test. The results in Table 6 show that 9% SDO passes the TFOT weight loss specification, as well as improves the viscosity of recycled asphalt cement. While the penetration is below the 85/100 specification, it is possible that either a soft flux can be used, or further addition of SDO can be utilized to soften to a penetration of 85 dmm.

One additional benefit of using SDO for rejuvenation is its property as an antistripping agent. A 9% blend of SDO into aged asphalt cement had a static immersion coverage of 100% on Jamieson aggregate. The unmodified, aged asphalt cement had a coverage of only 42%. The results of SDO rejuvenated asphalt cements in the thin film oven test are also encouraging. As shown in Table 6, when 9% SDO was added to an aged asphalt cement and subjected to the thin film oven test, a 60% retention of the penetration occurred along with a weight loss of 0.60%. Both meet the ASTM D-946 specification.

These results show the performance of SDO as a rejuvenating agent. Not only does it perform well for rejuvenation, softening, and asphaltene compatibility, it also improves the stripping resistance of the rejuvenated asphalt cement. This increases its value over other agents to recyclers of asphalt pavement. Further, it should be noted that the amounts of SDO used are reported as a fraction of the aged asphalt cement. While this may represent a small amount on the scale of recycled pavement, methods to contact the aged asphalt cement with SDO must be considered.

CONCLUSIONS

It has been demonstrated by extensive antistripping studies conducted on the different SDO samples supplied to ERL that the SDO antistripping properties are independent of the process used to produce the sludge derived oil (bench scale versus pilot scale), and relatively dependent on the sludge type (digested versus undigested). The digestion process removes some materials that would be converted to SDO in the oil from sludge process. The SDO from digested sludge also is less effective as an antistripping agent relative to the SDO from undigested sludge.

A 3% SDO concentration was found to be as effective as 5% SDO concentration for stripping inhibition. Furthermore, when SDO was used at 3% concentration, the A/C's properties (penetration, viscosity and weight loss after TFOT) were not modified as much as when a 5% concentration was used. If one would like to use 5% SDO, the starting asphalt cement should be in the 60/70 penetration grade to produce a final A/C in the 85/100 penetration range. A comparison of the performance of the year old SDO sample with a fresh sample at the 5% additive level showed no major difference confirming that the SDO is very stable over time and does not lose its beneficial properties.

The addition of SDO can be done either by the wet mode (standard method) in which the additive is blended with the A/C or by the dry mode in which the aggregates are prewetted with SDO before adding the A/C. In the latter case, asphalt engineering/performance tests would be required to confirm that this method does not affect the performance. This is being addressed in road pavement test strips.

The SDO Marshall stability (strength test) was found to be comparable to that of a commercial additive although a greater concentration of SDO is needed. Neither of these additives showed improvement or loss of stability over the commercial virgin asphalt used as control indicating no negative effect on the strength of the asphalt concrete.

Annual demand for antistripping agents for road asphalts in Ontario is valued at approximately \$1 million (6). It is estimated that up to 1000 t/a of SDO could be used in such an application. Initial experimentation has also shown that SDO shows promise as a rejuvenant for aged asphalt cement. Not only does SDO perform well for rejuvenation, softening, and asphaltene compatibility, it also improves the stripping resistance of the rejuvenated asphalt cement. This increases its value over other agents to recyclers of asphalt pavement. Recycling asphalt pavement is not a mature technology. Many opportunities exist to advance this technology. As the aggregate resources close to major centres become depleted, this technology will undoubtedly receive more attention.

ACKNOWLEDGEMENTS

The authors wish to thank P. Mourot and D. Martinoli of Enersludge Inc. and H. Campbell of WTC for their financial and technical support and their assistance in interpreting the results of this work. The authors also wish to thank J. Odgren of the Regional Municipality of Ottawa-Carleton's Material Testing Laboratory for technical support and interpretation of the Marshall Test portion of the research. Federal support of this work was provided through the Federal Program on Energy Research and Development (PERD).

REFERENCES

1. Campbell, H.W. and Bridle, T.R. "Sludge management by thermal conversion to fuels", Proc. of New Directions and Research in Waste Treatment and Residuals Management, Vancouver, 1985.
2. Campbell, H.W. and Martinoli, D.A. "A status report on Environment Canada's oil from sludge technology", Proc. of Status of Municipal Sludge Management for the 1990s, WPCF Specialty Conference, New Orleans, 1990.
3. Gearhart, J.A. and Nelson, S.R. "Upgrading heavy residuals and heavy oils with ROSE", Energy Processing/Canada, May-July, 1983.
4. Poirier, M.A. and Sawatzky, H. "The utilization of process residues for the production of road asphalt cements", Proc. of 30th Annual Conference of the Canadian Technical Asphalt Association, Moncton, 30, 42-58 (1990).
5. Stolle D.F.E. "Silane coupling agents to reduce moisture susceptibility of asphalt concrete", MTO Report #PAV-90-04, November 1990.
6. Kennepohl, G.J., MTO, personal communication, 1990.

Table 1 - ASTM asphalt cement specification tests

ASTM method	Test description
ASTM D-5	Penetration of bituminous materials
ASTM D-92	Flash Point, Cleveland Open Cup
ASTM D-113	Ductility of bituminous materials
ASTM D-1754	Effect of heat and air on asphaltic materials
ASTM D-2052	Solubility of asphalt materials in trichloroethylene
ASTM D-2170	Kinematic viscosity of asphalts
ASTM D-2171	Viscosity of asphalts by vacuum capillary viscometer

Table 2 - Atlanta SDO in asphalt cement

Test	Strp. Imm.	Penetration 4°C, 25°C, 30°C	Flash Point (°C)	Viscosity Absolute Kinematic 60°C 135°C	Ductility (cm)	TriCIEth Solubility (%)	THIN FILM OVEN TEST						
							Weight Loss (%)	Penetration 25°C (dmm)	Retained Penetration (%)	Viscosity Absolute Kinematic 60°C 135°C (P) (cSt)	Ductility (cm)	Strp. Imm.	
A/C# 88/100													
0% SDO	38	8, 96, 158	324	1573 332.1	+150	99.93	0.02	53	55.2	3178	446.2	+150	25
5% SDO	96	13, 156, 189	248	1044 228.0	+150	99.85	0.91	75	48.1	1756	340.3	+150	94
2% Redukote 82S	74	13, 121, 144	300	1043 278.0	+150	99.93	0.18	68	56.2	1915	387.3	138	87
1% Naaldad	94												
A/C# 150/200													
0% SDO	20	15, 174, 218	318	476.1 191.8	130	99.85	0.00	99	56.9	799.5	244.0		
5% SDO	95	19, 242, 301	284	315.1 141.8	+150	99.85	0.84	132	54.5	813.5	183.7	+150	95
2% Redukote 82S	85	16, 194, 292	304	389.4 168.8	+150	99.98	0.08	138	71.1	569.0	207.8	+150	95
1% Naaldad	87												
1% Alkazine 0	75												
A/C# 88/100													
0% SDO	39	8.83		392.0									
2% SDO	95	9.91	288	1292 327.0			0.30	62	68.1	3532	512.0		
1% Alkazine 0	80												
Spec ASTM D248													
85/100	+95*		>232	>280**	>100	>99	<0.85		>47			>75	
150/200	+95*		>220		>100	>99			>40				

*Spec ASTM D1864
**Spec MTO la-202

Lab2ed0.wk3

Table 3 - Performance of SDO in asphalt cement

Test	Penetration 4°C, 25°C, 30°C	Flash Point (°C)	Viscosity Absolute Kinematic 60°C 135°C	Ductility (cm)	TriCIEth Solubility (%)	THIN FILM OVEN TEST					
						Weight Loss (%)	Penetration 25°C (dmm)	Retained Penetration (%)	Viscosity Absolute Kinematic 60°C 135°C (P) (cSt)	Ductility (cm)	
A/C# 88/100											
0% SDO	7, 82, 135	292	1557 328.8	+150	99.86	0.00	58	71	3574	481.5	+150
3% SDO	11, 104, 204	244	1096 259.4	+150	99.80	0.72	62	60	2456	383.8	+150
5% SDO	11, 128, 238	226	768.4 227.2	135	99.89	1.24	68	54	2238	354.8	+150
0% SDO old	8, 96, 156	324	1573 332.1	+150	99.93	0.02	53	55	3176	446.2	+150
5% SDO old	13, 156, 189	248	1044 228	+150	99.85	0.91	75	48	1756	340.3	+150
A/C# 150/200											
0% SDO	12, 141, 253	286	716.2 237.0	149	99.61	0.01	79	56	1426	318.4	+150
3% SDO	15, 173, 307	288	510.6 192.2	128	99.83	0.80	88	57	1421	282.8	+150
5% SDO	17, 227, 372	232	420.2 186.5	115	99.89	1.24	107	47	977.6	254.4	+150
0% SDO old	8, 96, 156	324	1573 332.1	+150	99.93	0.02	53	55	3176	446.2	+150
5% SDO old	13, 156, 189	248	1044 228	+150	99.85	0.91	75	48	1756	340.3	+150

Table 4 - Marshall stability tests (MTO LS-263)

	Sample #	Stability (KN)	Flow (.001 in.)	V.M.A.* (%)	Air Voids (%)
Control	I A	11.225	9.50	15.09	6.00
	I B	11.002	9.90	14.88	6.20
	II A	12.622	---	13.57	4.88
	II B	12.958	11.00	13.61	4.96
	III A	13.972	10.12	14.33	5.56
	III B	12.292	10.72	15.25	6.45
5% SDO	I A	14.330	9.10	14.17	5.47
	I B	11.063	8.20	14.59	5.38
	II A	10.448	---	13.47	5.28
	II B	10.995	9.40	13.29	4.72
	III A	12.993	10.76	12.54	4.12
	III B	13.612	9.10	13.02	4.14
2% Redicote 82S	I A	6.687	2.80	18.46	2.58
	I B	6.689	3.00	16.35	2.59
	II A	12.017	9.40	14.14	5.83
	II B	10.585	10.50	14.38	6.28
	III A	12.545	8.34	14.40	6.34
	III B	14.784	9.09	13.83	5.78

* V.M.A. - Voids in mineral aggregates
 Calculated by the following formula: $V.M.A. = 100 - [C(100-AC)/G]$
 where C = Bulk specific gravity of compacted bituminous mixture
 AC = Wt % asphalt cement (A/C)
 G = Maximum specific gravity of aggregate, assumed at 2.70
 All mixes made with 5% by weight A/C - 85/100 penetration
 Coarse aggregate (>#4 US Sieve) - Jamieson [40 wt %]
 Fine aggregate (<#4 US Sieve) - Dibblec [60 wt %]

Table 5 - Comparison of penetration and viscosity in AAC² using different additives

	Penetration (dmm)		Kinematic viscosity (cSt)	
	4°C	25°C	100°C	135°C
AAC	7	30	11039	866
AAC + 2.1% SDO	7	40	6883	719
AAC + 6.0% SDO	7	50	4794	624
AAC + 12.2% SDO	11	98	4801	413
AAC + 22.0% Bow River 454°C	13	80	3079	287
Bow River 454°C	> 300	n/a ³	67	21
SDO	> 400	n/a	22	7

Table 6 - AAC properties before and after addition of SDO

A/C	SDO (%)	Viscosity @ 60°C (P)	Penetration @ 25°C (dmm)	TFOT wt loss (%)	Post TFOT		
					Viscosity @ 60°C (P)	Penetration @ 25°C (dmm)	Retained pen ⁴ (%)
AAC	0	29 720	32	0.03	45 210	-	-
AAC	9	5 330	65	0.60	9 583	39	60

² AAC: Aged asphalt cement

³ n/a: not analyzed

⁴ Pen: Penetration

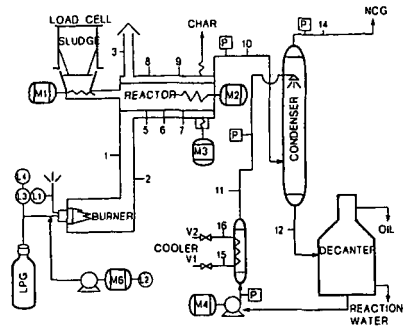


Fig. 1 - SCHEMATIC OF OFS PILOT PLANT, HAMILTON, ONTARIO

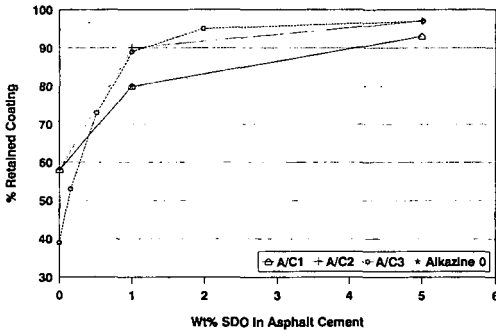


Fig. 2 - STRIPPING BY STATIC IMMERSION TEST

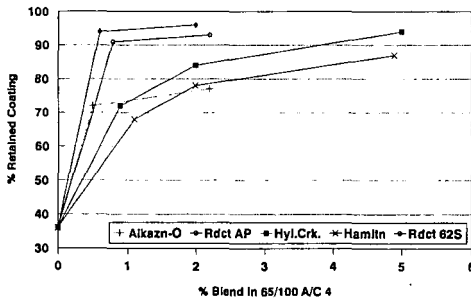


Fig. 3 - ANTISTRIPPING TEST ADDITIVE BLENDS VS RETAINED COATING

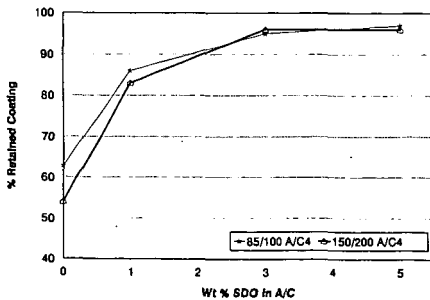


Fig. 4 - STRIPPING BY STATIC IMMERSION TEST

MANUFACTURE OF AMMONIUM SULFATE FERTILIZER FROM FGD-GYPSUM

M.-I.M. Chou, J.A. Bruinius, Y.C. Li, M. Rostam-Abadi, and J.M. Lytle
Illinois State Geological Survey
615 E Peabody Drive
Champaign, IL 61820

KEYWORDS: gypsum, ammonium sulfate, flue gas desulfurization

ABSTRACT

The goal of this study is to assess the technical and economic feasibility of producing marketable products, namely fertilizer-grade ammonium sulfate and calcium carbonate, from gypsum produced as part of lime/limestone flue gas desulfurization (FGD) processes. Millions of tons of FGD-gypsum by-product will be produced in this decade. In this study, a literature review and bench-scale experiments were conducted to obtain process data for the production of marketable products from FGD-gypsum and to help evaluate technical and economic feasibility of the process. FGD-gypsum produced at the Abbott power plant in Champaign, IL was used as a raw material. The scrubber, a Chiyoda Thoroughbred 121 FGD, produced a filter cake product contains 98.36% gypsum ($\text{CaSO}_4 \cdot 2\text{H}_2\text{O}$), and less than 0.01% calcium sulfite (CaSO_3). Conversion of FGD-gypsum to ammonium sulfate were tested at temperatures between 60 to 70°C for a duration of five to six hours. The results of a literature review and preliminary bench-scale experiments are presented in this paper.

INTRODUCTION

The 1990 amendments to the Clean Air Act mandate a two-stage, 10-million ton reduction in sulfur dioxide emissions in the United States¹. Plants burning high sulfur coal and using FGD technologies must also bear increasingly expensive landfill disposal costs for the solid waste produced². The FGD technologies would be less of a financial burden if successful commercial uses were developed for the gypsum-rich by-products of the wet limestone scrubbing.

The degree to which FGD-gypsum is commercially used depends on its quality. Currently, high-quality FGD-gypsum with purity greater than 94% is used mainly to manufacture construction materials, i.e. stucco and gypsum-plaster, gypsum wall boards, and cement³. The amount of high quality FGD gypsum could exceed the current demand of the FGD-gypsum industry. Conversion of FGD-gypsum to marketable products could be a deciding factor in the continued use of high-sulfur Illinois coals by electric utilities. One approach is to produce cost-competitive ammonium sulfate fertilizer and commercial-grade calcium carbonate from FGD-gypsum.

Ammonium sulfate is a valuable source of both nitrogen and sulfur nutrients for growing plants. There is an increasing demand for sulfur in the sulfate form as a plant nutrient because of diminished deposition of atmospheric sulfur compounds from flue gas emissions and more sulfur is taken up by plants produced in high yields⁴. Also, the trend of using high-nitrogen content fertilizers has pressed incidental sulfur compounds out of traditional fertilizer. The current market for ammonium sulfate in the United States is about two million tons per year. It is anticipated that 5 to 10 million tons of new ammonium sulfate production may be required for fertilizer markets annually to make up for the loss of sulfur deposition from the increased restriction on acid-rain. The fertilizer industry appears ready to accept an added source of fertilizer grade ammonium sulfate to supply sulfur in NPK fertilizer blends⁵.

In Phase-I of this study, a literature review and a series of bench-scale experiments were conducted to obtain process data for the production of ammonium sulfate from FGD-gypsum and to help evaluate technical and economic feasibilities of the process.

EXPERIMENTAL PROCEDURES

Sample of FGD-gypsum and methods of analyses - The Abbott power plant in Champaign, Illinois operates a Chiyoda Thoroughbred 121 FGD-desulfurization system which produces one ton of gypsum for every ten tons of coal burned. The FGD-gypsum sample collected was dried in ambient air for two to four days. The particle size distributions of the sample were determined using both manual and instrumental methods. In the manual method, the sample was wet-sieved through a 100 mesh (149 μm) screen and then a 200 mesh (74 μm) screen. The weight % of the size-fractional samples were determined after drying. In the

instrumental method, a Micro Trac II analyzer was used to determine the mean and standard deviation of the particle diameter by means of laser light scattering.

The amounts of free water (released at 45°C) and combined water (released at 230°C for gypsum), calcium oxide (CaO), magnesium oxide (MgO), and carbon dioxide in the sample were determined by the ASTM method C471. Based on these analytical results, the compositions were calculated in terms of %CaCO₃, %MgCO₃, %CaSO₄, %CaSO₄·2H₂O, and %(NH₄)₂SO₄. Thermogravimetric analysis (TGA) was conducted under an air flow of 50 mL/min with programmed heating from room temperature to 900°C at 10°C/min. The weight loss profile was used for preliminary estimates of purity and composition of gypsum.

Conversion of FGD-gypsum to ammonium sulfate and calcium carbonate - The batch, bench-scale reactor system consisted of a 1000-mL, three-neck, round-bottomed flask fitted with a mechanical stirrer, a condenser, and a thermometer. An autotransformer and heating mantle were used to control the reaction temperature. The important reaction for producing ammonium sulfate from the FGD-gypsum is the reaction between ammonium carbonate and calcium sulfate. Two sets of experiments were conducted in this study. In the first set of experiments, the gypsum reacted with reagent-grade ammonium carbonate in a liquid medium. In the second set of experiments, ammonium carbonate, formed by the reaction of ammonia and carbon dioxide in a liquid medium reacted with suspended gypsum. The procedures for the experiments are outlined below.

FGD-gypsum was added to an ammonium carbonate solution (prepared by dissolving reagent-grade ammonium carbonate in 500 mL of distilled water) in the 1000-mL reaction flask. The temperature of the stirred mixture was raised from room temperature to the reaction temperature and maintained at that temperature for a range of pre-determined times. The solution which contained the ammonium sulfate product was separated from the solid byproduct, calcium carbonate, by vacuum filtration. The filtrate plus the rinsing, a total of about 600 mL of the liquid, was concentrated to a volume of about 150 mL in a constant temperature water bath. The residual concentrate was kept at room temperature to form ammonium sulfate crystals. The condensation and crystallization steps were repeated until no more crystal could be produced. The combined product was dried under ambient air before determining the total weight.

In the second set of experiments, ammonium carbonate was formed by the reaction of ammonia and carbon dioxide in a liquid medium, which was then allowed to react with FGD-gypsum in suspension. After removal of the calcium carbonate, the ammonium sulfate is recovered in a similar manner by filtration, evaporation and crystallization.

The ammonium sulfate produced was analyzed by melting point determination, chemical analysis and TGA analysis. The yield of the ammonium sulfate produced was obtained based on its theoretical yield from a total conversion of calcium sulfate feed. The purity of the ammonium sulfate produced was determined by chemical analysis of the nitrogen content using methods described by the Association of Agriculture Chemists (AOAC) and American Water Works Association (AWWA) procedure, and by ASTM method C-471. The calcium carbonate by-product was dried and subjected to TGA analyses to determine its purity and composition of unreacted gypsum.

RESULTS AND DISCUSSIONS

Characterization of the FGD-gypsum sample - The data on particle size distribution obtained by passing the gypsum sample through a series of screens and by Micro Trac II particle-size analyzer are shown in Table 1. About 84% of the sample has particle-size smaller than 74 μm (200 mesh), and about 99% of the sample has particles of smaller than 149 μm (100 mesh). The results of chemical analyses and the calculations following ASTM method C-471 are shown in Table 2. The FGD-gypsum sample has more combined water (water of hydration) than free moisture and has 98.36% gypsum (CaSO₄·2H₂O) with less than 0.01% of calcium sulfite (CaSO₃). The TGA curve of the gypsum sample is shown in Figure 1. All weight loss occurred between 98°C and 207°C (peak at 158.65°C). This weight loss is related to removal of the water of hydration from gypsum. No further thermal decomposition occurred to a temperature of 900°C.

Literature review - The chemistry of the process and process conditions⁶ were reviewed. The literature study showed that the production of ammonium sulfate from natural gypsum, ammonium, and carbon dioxide, known as the Merseburg Process, has been tried in England⁷ and India⁸ in 1951 and 1967, respectively. The process was proven to be

commercially feasible. The Merseburg Process for manufacturing ammonium sulfate from gypsum is based on the chemical reaction between gypsum and ammonium carbonate. Ammonium carbonate is formed by the reaction of ammonia and carbon dioxide in aqueous solution. The reaction produces insoluble calcium carbonate and an ammonium sulfate solution. The reason it is not currently used is the cost of natural gypsum and the availability of an economical source of carbon dioxide.

In the early 1960's, the chemistry of the Merseburg Process was carefully studied and partially developed in the U.S.. At that time the Tennessee Valley Authority (TVA) studied a process in which ammonium phosphate was produced using ammonium sulfate and phosphate rock as starting materials. In the process, phosphate rock was extracted with nitric acid. The extract was allowed to react with ammonium sulfate to produce ammonium phosphate. Gypsum was produced as a by-product. To minimize the costs of ammonium phosphate conversion, TVA adopted the Merseburg Process and developed a single-stage reactor both in bench scale⁹ and in pilot scale¹⁰ operations. The purpose was to recover the by-product gypsum and use it to regenerate ammonium sulfate for the starting material. In the regeneration, the by-product gypsum and ammonium carbonate were premixed before entering the reactor. Residence times of 0.5, 1, and 3 hours at 125°F (52°C) and 140°F (60°C) were tested, and conversions of greater than 95% were achieved⁹. Typical operating conditions in the pilot plant were 120°F (49°C), 2 hours residence time, and ammonium carbonate feed at or above 105% stoichiometric requirement, and the conversion was 98%¹⁰.

Bench scale testing for ammonium sulfate production - The important reaction for producing ammonium sulfate from the FGD-gypsum is the reaction between ammonium carbonate and calcium sulfate. Two sets of experiments (see experimental procedures section) were conducted in this study. The reaction conditions, amounts of reactants, and the properties of products for the two sets of experiments are listed in Table 3. The ammonium sulfate produced was confirmed both by comparing its melting point with that of a commercial standard and by examining chemical analysis data and TGA data. Based on the weight of the ammonium sulfate produced and its theoretical yield from a total conversion of calcium sulfate feed, a yield of up to 83% and a purity of up to 99% for the ammonium sulfate production was achieved. A mass balance calculation for calcium and sulfur in gypsum was conducted on experiment run No. 5 (Table 3). The results show a recovery of 98% for calcium in calcium carbonate and a recovery of 81% for sulfur in ammonium sulfate were obtained. The TGA curve for calcium carbonate produced in one of the residues is shown in Figure 2. The graph shows a weight loss occurring between 600°C and 770°C. This is attributed to the evolution of carbon dioxide from decomposing calcium carbonate. A typical TGA curve (Figure 3) of the ammonium sulfate produced shows a total decomposition of the sample with a maximum weight loss at 418.3°C.

In summary, the results of these preliminary laboratory experiments suggest that high quality ammonium sulfate can be produced from the FGD-gypsum sample obtained from the Abbott power plant.

ACKNOWLEDGEMENT & DISCLAIMER

This report was prepared by M.-I. M. Chou and the ISGS with support, in part, by grants made possible by U.S. department of Energy (DOE) Cooperative Agreement Number DE-FC22-PC92521 and the Illinois Coal Development Board (ICDB) and the Illinois Clean Coal Institute (ICCI). Neither authors nor any of the subcontractors nor the U.S. DOE, ISGS, ICDB, ICCI, nor any person acting on behalf of either assumes any liabilities with respect to the use of, or for damages resulting from the use of, any information disclosed in this report. The authors would like to acknowledge D.F. Fortik of the Abbott Power Plant for supplying the FGD-gypsum sample and the project manager D.D. Banerjee of the ICCI.

REFERENCES

1. E. Claussen, "Acid Rain: The Strategy," Office of Communications and Public Affairs, EPA Journal, Washington DC, Jan./Feb. 1991, vol. 17, no. 1.
2. R.E. Bolli and R.C. Forsythe, "Ohio Edison Company's Clean Coal Technology and Waste Utilization Programs," EPRI 1990 SO₂ Control Symposium, vol. 1, 3b.
3. S.K. Conn, M.G. Vacek, and J.T. Morris Jr., "Conversion from disposal to commercial grade gypsum; An alternative approach for disposal of scrubber wastes." EPRI 1993 SO₂ Control Symposium, vol. 3, 8b.
4. R.G. Hoeft, J.E. Sawyer, R.M. VandenHeuvel, MA. Schmitt, and G.S. Brinkman,

- Corn response to sulfur on Illinois soils, *J. Fert.*, 2:95-104, 1985.
- N.W. Frank and S. Hirano, "Utilization of FGD Solid Waste in the Form of By-product Agricultural Fertilizer," EPRI 1990 SO₂ Control Symposium, vol. 1, 3b.
 - Kirk-Othmer, *Encyclopedia of Chemical Technology*, fourth edition, vol. 2, 706, John Wiley & Sons, New York, 1992.
 - Higson, G.I., *The Manufacture of Ammonium Sulphate from Anhydrite*, Chemistry and Industry, 750-754, September 8, 1951.
 - Nitrogen, Conversion of Gypsum or Anhydrite to Ammonium Sulfate, Nitrogen, 46, March/April 1967.
 - Blouin, G.M., O.W. Livingston, and J.G. Getsinger, Bench-Scale Studies of Sulfate Recycle Nitric Phosphate Process, *J. Agr. Food Chem.*, vol. 18, 313-318, 1970.
 - Meline, R.S., H.L. Faucett, C.H. Davis, and A.R. Shirley Jr., Pilot-Plant Development of the Sulfate Recycle Nitric Phosphate Process, *Ind. Eng. Process Des. Develop.*, vol. 10, 257-264, 1971.

Table 1. Results of particle size analysis of the FGD-gypsum

Size	%
> 149 μm^1	0.97
149-74 μm^1	15.40
< 74 μm^1	83.60
average diameter (μm) ²	73.88
standard deviation ²	35.63

¹By sieve analysis; ²By Micro Trac II

Table 2. Results of ASTM chemical analysis of the FGD-gypsum

Analytes	Composition in wt. % moisture free basis
combined water	20.59
CaO	32.92
MgO	0.01
SO ₄	54.90
SO ₃	<0.01
CO ₂	0.71
NH ₃	<0.01
Free Moisture	<0.01
Calculated Values	
CaSO ₄ ·2H ₂ O	98.36
CaCO ₃	1.60
CaSO ₄	<0.01
CaSO ₃	<0.01
MgCO ₃	0.01
(NH ₄) ₂ SO ₄	<0.01

Table 3. Reaction conditions and the results of final product and by-product analyses

Run number	Run Conditions	¹ Mole ratio	CaCO ₃		(NH ₄) ₂ SO ₄		
			² Wt% in residue	³ Calculated yield	⁴ purity	³ Calculated yield	⁵ m.p. (°C)
1	70°C 5hr	1.56	97	ND	ND	ND	242
2	70°C 6hr	1.59	86	ND	95	82	237
3	70°C 6hr	1.33	81	81	ND	83	241

Run number	Run conditions	NH ₃ mole/hr	CO ₂	CaCO ₃		(NH ₄) ₂ SO ₄		
				² wt% in residue	³ calculated yield	⁴ purity	³ Calculated yield	⁵ m.p. (°C)
4	60°C 4hr ⁶	1.50	1.25	ND	ND	99	58	240
5	65°C 6hr ⁶	1.25	1.00	94	104	95	83	241
6	70°C 6hr ⁶	1.25	1.00	ND	ND	90	76	237

¹The mole ratio of (NH₄)₂CO₃ to CaSO₄·2H₂O; ²Wt % CaCO₃ in residue by TGA;

³Based on theoretical yield from FGD-gypsum feed;

⁴Wet chemical analysis by ASTM C-471 and AWWA procedures;

⁵Melting point for the standard is 240°C; ⁶1.95 mole of gypsum used.

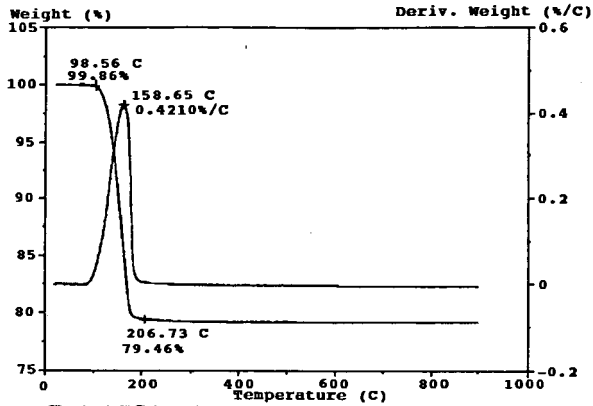


Figure 1: Typical TGA weight loss profile and first derivative for FGD-gypsum from the Abbott Plant.

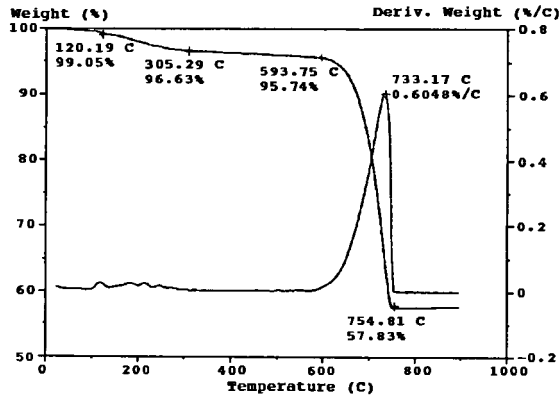


Figure 2: Typical TGA weight loss profile and first derivative for solid by-product (CaCO_3) from the ammonium sulfate production.

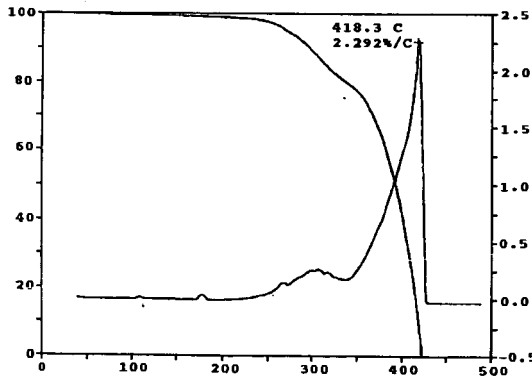


Figure 3: Typical TGA weight loss profile and first derivative of ammonium sulfate produced.

TECHNO-ECONOMIC EVALUATION OF WASTE LUBE OIL RE-REFINING IN SAUDI ARABIA

Mohammad Farhat Ali, Abdullah J. Hamdan and Faizur Rahman
DEPARTMENT OF CHEMISTRY
King Fahd University of Petroleum & Minerals
Dhahran, Saudi Arabia

Keywords: Waste Lube Oil, Re-refining, Economics

INTRODUCTION

About 80 million gallons of automotive lubricating oils are sold in Saudi Arabia. Much of this oil, after use, is actually contributing to the increased pollution of land because of indiscriminate dumping. Any scheme of secondary use of the waste lube oils would be of interest both for conservation of energy resources and for protection of environment. This paper discusses the secondary use for the used automotive lubricating oils. Process technology of Meinken, Mohawk and KTI were selected for the techno-economic feasibility study for re-refining used oil. Profitability analysis of each process is worked out and the results are compared.

In many countries the re-refining of the used oils has become an important industry. The objective of recovering high quality raffinates is attained through the use of widely differing techniques.

The processes concerned can be classified according to the chemical or physical method of used-oil pretreatment selected. Meinken process is based on chemical pretreatment whereas, both Mohawk and KTI processes employ physical methods involving distillation and eliminates the use of sulfuric acid thus providing a facility for safer operation than Meinken.

The plant capacity of two existing units in Jeddah are 10,000 TPA and 80,000 TPA re-refining of waste oil. We selected a plant of 50,000 TPA waste oil re-refining for economic study of these three processes.

Both Mohawk and KTI have been running full range plants in different parts of the world and appear to be efficient and viable. Meinken have successfully implemented more than 60 used oil re-refining plants world wide including Kuwait Lube Oil Company, Iran Motor Oil Company, Saudi Lube Oil Company Limited, Jeddah, and Lube Oil Co. Ltd., Jeddah.

PROCESS TECHNOLOGIES

Meinken Process

The used oil is supplied to the re-refinery by railway tankers, road tankers or in barrels. Before the used oil flows into the waste oil storage tanks, it passes through the filters to remove solid impurities. A block flow diagram of re-refining process is shown in Figure 1.

Meinken process is based on chemical pretreatment [1]. The dewatered oil is treated with sulfuric acid (96 %) and the acid refined oil is vacuum distilled to separate lube base oil from the low boiling spindle oil and gas oil. With sulfuric acid treatment it is necessary to dehydrate the feedstock completely before subjecting it to acid treatment to prevent dilution of the concentrated sulfuric acid. On the other hand, there is no need to remove crankcase "dilution" or fuel components ahead of the acid-treating step, since these could be conveniently stripped from the hot oil in the subsequent clay contacting step. Their presence during acid treatment reduces the viscosity of the oil and thereby increase the ease of separating the acid sludge. However, the sulfuric acid - treatment and clay addition produce waste streams like acid tar and spent clay resulting in a problem of waste disposal. In spite of the disposal problem associated with Meinken process, the Meinken technology appears to be very popular. At present, there are about 60 such refiners around the world using the same system. New refineries of this type are in various stages of construction and planning in Kuwait, Saudi Arabia, UAE, Oman and India manifesting the technology to be well proven and widely accepted.

Mohawk Process

A simplified block flow diagram of the Mohawk-CEP process is shown in Figure 2. This is claimed by the licensors to be the newest and yet proven high-efficiency re-refining technology. Mohawk technology has been licensed to Chemical Engineering Partners, a private chemical engineering design company based in California, U.S.A.

The first stage of the process removes water from the feedstock [5,6]. The second stage of the process is distillation, at this step light hydrocarbons are removed resulting in a marketable

fuel by-product. The third stage, evaporation, vaporizes the base oil, separating it from the additives, leaving behind a by-product called residue. This residue is used in asphalt industry. The final processing stage is hydrotreatment which results in a high quality base oil.

The Mohawk process features continuous operation, low maintenance, longer catalyst life span, reduced corrosion, and proven technology.

KTI Process

Kinetic Technology International (KTI) of the Netherlands, in close cooperation with Gulf Science and Technology Co. (Pittsburgh, Pa.) has developed a new re-refining process for all types of waste lubricating oils [5,10].

The KTI waste lube oil re-refining process involves a series of proprietary engineering technologies that affords high economic returns without resulting in environmental loads. The main features of the KTI process include : (a) high recovery yield up to 95 % of the contained lube oil; (b) excellent product quality; (c) flexible operation with wide turndown capability; (d) no requirement for discharging chemicals or treating agents; (e) absence of non commercial by-products; and (f) reliable, inexpensive treatment of waste water contained in the wasted lube oil.

The important steps of this process are as follows. Atmospheric distillation, which removes water and gasoline. Vacuum distillation using special wiped film evaporators separates lube oil from heavy residue containing metals and asphaltenes. The next step is hydrofinishing of lube oil. Hydrogen rich gas is mixed with the oil and heated before passing through the reactor. The treated oil is then steam stripped or fractionated into cuts using a vacuum in order to obtain the right specification.

ECONOMIC EVALUATION

Capital Investment

The total fixed capital investment to process 50,000 TPA of waste oil was obtained from Meinken [1] and Mohawk [6] in 1991. Location factor of 1.25 was used to estimate the fixed capital costs for Saudi location [2]. Table 1 lists the total fixed capital investment estimated for both the technologies. Working capital for the re-refinery was estimated by itemizing the production costs components [12]. It varies with changes in raw material prices, product selling price and so on.

Economic evaluation of KTI process could not be carried out because of non-availability of complete cost data.

Production costs

Production costs consists of direct costs, indirect costs and general expenses.

Direct cost includes expenses incurred directly from the production operation. These expenses are : raw materials (including delivery), catalysts and solvents, utilities, operating labor, operating supervision, maintenance and repairs, operating supplies, royalties and patents.

Raw material prices were estimated from F.O.B. prices in Germany in September 1991 [1,3] and includes \$90.0 per ton for shipping. Local price was used for sulfuric acid. Collection cost of waste oil in Jeddah [1], Saudi Arabia was estimated as \$53.52 per ton. By-product(gas oil) price \$110 per ton was taken from Petroleum Economist[9], for Caltex, Bahrain location. By-product asphalt price \$130.0 per ton was taken from CMR [3], but reduced by 15% as it needs some more processing. If the asphalt residue can not be sold at international price due to low demand in this region, its price has to be further reduced. For economic analysis purposes, the price of asphalt residue was still lowered by 50 %. This is an approximation and the price used finally in the calculations is \$55.0 per ton of asphalt residue.

The raw materials, utilities, and manpower requirements are given in Table 2 which were obtained from Meinken [1] and Mohawk [8]. Table 3 lists raw materials, utilities and manpower costs estimated for Saudi Arabian location [2,11]. Natural gas price was taken as \$0.5 per million Btu [2] and the benefit of low price of natural gas is reflected in utilities costs such as electricity and steam. However, process water is expensive in Saudi Arabia because it is produced from desalination plants.

Operating costs which includes operating labor, supervision, maintenance and repairs and indirect costs which includes overheads, storage and insurance, and general expenses were estimated according to the standard procedures [7,13,14].

Summation of all direct costs, indirect costs and general expenses results in a production cost. Table 4 illustrates production cost of re-refining waste oil resulted from the two technologies. The estimated production cost for Meinken process was \$ 348.8 per ton and for Mohawk process it is \$ 198.4 per ton of re-refined oil.

For Meinken process the raw materials cost is about 54 % of the production cost. Utilities is 3.0 %, operating cost is 17.2 %, total indirect costs is 20.4 % and general expenses about 7.4 % of the total product cost. The share of raw materials cost in the total product cost is dominant.

In case of Mohawk process the raw materials cost is about 42.7 % of the total product cost. By-products are 12.4 %, utilities are 8.8 %, operating cost 23.0 %, total indirect costs are 25.4 % and general expenses are 12.5 % of the total product cost. So, the production cost will be sensitive to raw materials prices and sensitivity analysis was performed for different raw materials price.

Profitability Analysis

The profitability of an industrial opportunity is a function of major economic variables such as product selling price, raw materials prices, capital investment, energy prices and so on. Year-by-year cash flow analysis have been carried out using assumptions and financial arrangements described in Table 5.

From the analysis of production costs (Table 4) components, it is obvious that the raw materials cost is the dominant item. So, sensitivity analysis were performed for 15 % lower and 15 % higher raw materials prices than prevalent in September 1991.

Since the re-refined oil is not segregated into different neutral oils and bright stock, following typical composition was assumed: 10 % 300 SN, 80 % 500 SN and 10 % bright stock. Based on LUBREF, Jeddah [4] base oil prices of various grades an estimated selling price of \$415.60 per ton is used in the financial analysis.

The year-by-year cash flow analysis for international raw materials prices (base case) in September 1991 and for 15 % lower and 15 % higher raw materials prices have been carried out. The results of cash flow analysis are summarized in Table 6. Figure 3 shows the effect of raw materials prices on internal rate of return (IRR).

The total fixed capital investment is very high for Meinken process (28.750 million \$) as compared to Mohawk process (17.713 million \$). The working capital amounts to a high value of 4.998 million U.S. Dollars for Meinken as compared to relatively low value of 3.050 million Dollars for Mohawk.

The payback period(PBP) and break-even-point (BEP) for Meinken Process are high as expected compared to Mohawk process, which are 8.16 years and 53.8 % of the full production. The PBP for Mohawk is 1.40 years, and BEP is 28.65 %. The IRR for Meinken and Mohawk are estimated to be 11.24 % and 45.36 %. Thus, the total positive annual cash flow for Mohawk process appears to be more attractive than that for Meinken. The high profitabilities of Mohawk process are due to lower capital costs as a result of (i) excluding hydrogen plant and (ii) possibly due to relatively not well established technology as compared to Meinken process.

The main disadvantage of Mohawk process is that, the plant has to be located near a refinery or petrochemical plant (because of hydrogen supply) to be able to realize such high profitabilities. If the facilities are to be provided with an independent hydrogen plant, then the capital costs may go up significantly and subsequently profitabilities will be dropped.

ACKNOWLEDGEMENT

The investigators wish to acknowledge King Abdul Aziz City for Science and Technology (KACST) for funding this Research Project (AR-10-60). The facilities and support provided by the Department of Chemistry and the Research Institute of King Fahd University of Petroleum and Minerals (KFUPM) is also gratefully acknowledged.

REFERENCES

1. B. Meinken, Private Communication, B. Meinken Project and Construction Management Consultants, Haltern, Germany, 1991.
2. SRI, PEP Yearbook International, Volume 1, SRI International Menlo Park, California, U.S.A., 1989.

3. Chemical Marketing Reporter, Schnell Publishing Company, Inc., New York, U.S.A., September 1991.
4. LUBEREF, Private Communication, Petromin Lubricating Oil Refining Company, Jeddah, Saudi Arabia, 1991.
5. Ali, M. F. and Hamdan, A. J. Studies on Used Lubricating Oil Recovery and Re-refining, Third Progress Report, KACST AR-10-60, KFUPM, Dhahran, 1990.
6. Magnabosco, L.H., M. Falconer and K. Padmanbhan, The Mohawk-CEP Re-refining Process, The Proceedings of Sixth International Conference on used oil Recovery and Reuse, San Francisco, California, May 28-31, 1991.
7. Garrett, D.E., Chemical Engineering Economics, Van Nostrand Reinhold, New York, U.S.A., 1989.
8. Mohawk, Private Communication, Mohawk Lubricants, A Division of Mohawk Oil Co. Ltd., Burnaby, B.C., Canada V5G 4G2, 1991.
9. Petroleum Economist, p.31, June 1991.
10. KTI, Waste Lube Oil Re-refining for King Fahd University of Petroleum and Minerals, Dhahran, Document No. 10091, Kinetic Technology International Corp., California, U.S.A., 1989.
11. TECNON, List of Heavy Petrochemical Industries for Royal Commission for Jubail and Yanbu, Madinat Yanbu Al-Sanaiyah, K.S.A., TECNON (UK) LTD., Petrochemicals Marketing and Planning Consulting Services, London, U.K. 1988.
12. Bechtel, L.R., Estimate Working Capital Needs, Chemical Engineering, 67 (4): 127 1960.
13. Axtell, O., Economic Evaluation in the Chemical Process Industries, John Wiley and Sons, New York, U.S.A., 1986.
14. Ulrich, G.D., A Guide to Chemical Engineering Process Design and Economics, John Wiley and sons, New York, U.S.A., 1984.

Table 1. Capital investment of 50,000 TPA waste oil re-refining plant in Saudi Arabia.

Process Technology	Total Fixed Capital in 1991 (Million US \$)
Meinken, Germany	28.750
Mohawk, Canada	17.713

Table 2. Raw materials utilities and manpower requirements per ton of product.

	Meinken process	Mohawk process
Raw Materials:		
• Waste oil, ton	1.266	1.343
• Sulfuric Acid, ton	0.095	-
• Activated clay, ton	0.049	-
• Lime, ton	0.214	-
• Ammonia water(23%), ton	0.008	-
• Catalyst, kg	-	3.76
By Products:		
• Gas oil, ton	- 0.060	- 0.135
• Asphalt, ton	-	- 0.176
Utilities:		
• Fuel oil, ton	0.075	0.116
• Cooling water, ton	-	2.003
• Process water, ton	75.000	97.020
• Hydrogen, ton	-	0.003
• Steam, ton	-	0.667
Manpower:		
• Total men for 3 shifts	33	31

(-ve) Sign indicates by-product

Table 3. Raw materials, utilities and manpower costs in Saudi Arabia.

Item	Cost (\$/unit)
Raw Materials:	
• Waste oil, ton	53.52
• Sulfuric Acid, ton	160.00
• Activated sludge, ton	673.00
• Lime, ton	316.00
• Ammonia water (23%),ton	387.00
• Catalyst, kg	3.41
Utilities:	
• Fuel oil, ton	110.00
• Cooling water, ton	0.019
• Process water, ton	0.803
• Electricity, Kwh	0.015
• Hydrogen, ton	65.000
• Steam, ton	4.630
Manpower:	
• One man year (\$/year)	18,000

Source: [1, 2, 3, 11]

Table 4. Production cost data.

Parameter	Meinken Process	Mohawk Process
Direct Costs:		
• Raw materials	188.21	84.70
• By-products	-6.64	-24.52
• Operating Cost	70.63	63.08
Indirect Cost	71.03	50.34
General Expenses	25.56	24.82
Total production cost	348.79	198.41

Table 5. Basis of financial calculations.

Item	Calculated Basis
Project life	20 years
Construction period	3 years
Depreciation method	Straight line
Salvage value	Zero
Equity/SIDF loan	50% each
SIDF Loan fee	3%
Loan payment	7 equal installments starting 2 years after plant start-up
Tax rate	2.5 %
Inflation	0.0 %
Capital expenditure:	
• 1st year	20% of fixed capital
• 2nd year	45% of fixed capital
• 3rd year	35% of fixed capital plus working capital
Capacity utilization:	
• 1st year	60%
• 2nd and subsequent years	100%

Table 6. Profitability of re-refining 50,000 TPA waste oil in Saudi Arabia (1000 \$)

	Meinken Process	Mohawk Process
Total fixed capital	28,750	17,713
Working capital	4,999	3,111
SIDF loan	16,875	11,356
Annual variable expenses	7,587	2,873
Annual fixed expenses	4,746	3,852
Annual sales	16,410	15,377
Payback period (years)	8.2	1.4
Break-even-point (% capacity)	53.8	28.7
IRR (%/year)	11.2	45.4

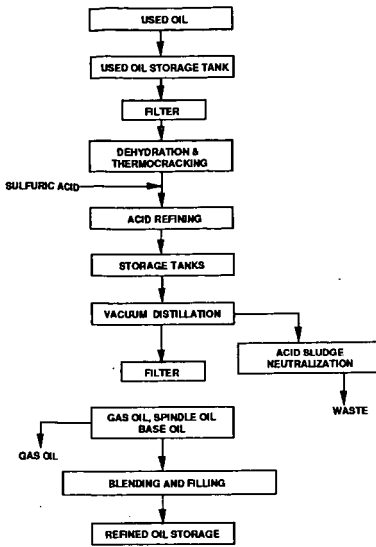


Figure 1. Block flow diagram of Re-refining of used oil by Meinken process

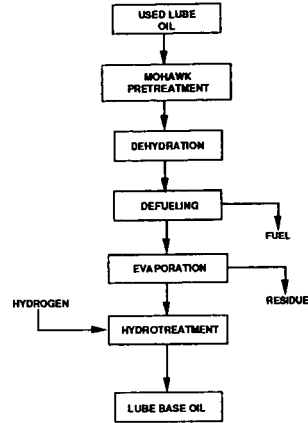


Figure 2. Block flow diagram of Re-refining of used oil by Mohawk-CEP process.

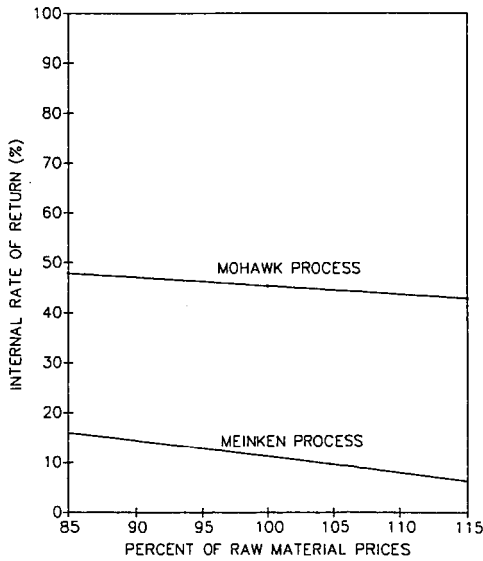


Figure 3. Effect of raw material prices on IRR.